

Binary Gaussian Copula Synthesis: A Novel Data Augmentation Technique to Advance ML-based Clinical Decision Support Systems for Early Prediction of Dialysis Among CKD Patients

Hamed Khosravi¹, Srinjoy Das², Abdullah Al-Mamun³, Imtiaz Ahmed^{4*}

¹*Department of Industrial & Management Systems Engineering, West Virginia University, Morgantown, WV 26505, Email: hk00024@mix.wvu.edu*

²*School of Mathematical & Data Sciences, West Virginia University, Morgantown, WV 26505, Email: srinjoy.das@mail.wvu.edu*

³*Department of Pharmaceutical Systems and Policy, School of Pharmacy, West Virginia University, Morgantown, WV 26505, Email: mohammad.almamun@hsc.wvu.edu*

⁴*Department of Industrial & Management Systems Engineering, West Virginia University, Morgantown, WV 26505, Email: imtiaz.ahmed@mail.wvu.edu*

**Corresponding Author: imtiaz.ahmed@mail.wvu.edu*

Abstract: The Center for Disease Control estimates that over 37 million US adults suffer from chronic kidney disease (CKD), yet 9 out of 10 of these individuals are unaware of their condition due to the absence of symptoms in the early stages. It has a significant impact on patients' quality of life, particularly when it progresses to the need for dialysis. Early prediction of dialysis is crucial as it can significantly improve patient outcomes and assist healthcare providers in making timely and informed decisions. However, developing an effective machine learning (ML)-based Clinical Decision Support System (CDSS) for early dialysis prediction (i.e., 90 days before initiation) poses a key challenge due to the imbalanced nature of data (i.e., with far fewer cases of dialysis patients compared to non-dialysis CKD patients). This data imbalance hinders the ability of ML models to accurately predict early dialysis. To address this challenge, this study evaluates various data augmentation techniques to understand their effectiveness on real-world datasets. We propose a novel approach named Binary Gaussian Copula Synthesis (BGCS). BGCS is tailored for binary medical datasets and excels in generating synthetic minority data that mirrors the distribution of the original data. BGCS enhances early dialysis prediction by outperforming traditional methods in detecting dialysis patients. It consistently leads to superior performance across models, significantly improving over real data. For the top-performing ML model, Random Forest, BCGS achieved a 72% improvement, surpassing the state-of-the-art (SOTA) augmentation approaches. However, it's noteworthy that all SOTA augmentation methods demonstrated enhancements over situations with no augmentation. Additionally, we present a ML-based CDSS, designed to aid clinicians in making informed decisions. This system utilizes decision tree models, which are widely adopted in healthcare settings for their interpretability. CDSS is developed to improve patient outcomes, identify critical variables, and thereby enable clinicians to make proactive decisions, and strategize treatment plans effectively for CKD patients who are more likely to require dialysis in the near future. Through comprehensive feature analysis and meticulous data preparation, we ensure that the CDSS's dialysis predictions are not only accurate but also actionable, providing a valuable tool in the management and treatment of CKD.

Keywords: Chronic kidney disease, Dialysis, Clinical Decision Support Systems, Data Augmentation, Binary Gaussian Copula Synthesis (BGCS)

1. Introduction

In the field of data science and machine learning (ML), the presence of imbalanced class labels in training datasets poses a significant challenge for classification tasks across various applications [1]. This issue occurs when certain classes in a dataset are represented by a disproportionately high number of instances compared to others [2]. It is observed that most ML algorithms struggle with accurately classifying data from such imbalanced datasets [3,4]. Typically, standard classifiers are biased towards classes with more instances [5], often treating data from minority classes as noise and overlooking it [6]. Consequently, instances belonging to these minority classes are more prone to misclassification compared to those from majority classes [7,8]. Imbalanced datasets are a frequent occurrence in real-world scenarios, including applications like predicting failures in manufacturing equipment [9], identifying spam emails [10], detecting fraudulent credit card activities [11], and diagnosing medical conditions [12]. Medical datasets frequently exhibit imbalanced class distributions, a situation that presents a considerable challenge for ML algorithms in disease classification tasks. This imbalance, often marked by a pronounced disparity between classes, is a typical scenario in medical contexts [13,14], especially in the analysis of electronic health records [15,16]. In these datasets, prevalent medical conditions are usually overrepresented, whereas rare diseases tend to be underrepresented. As a result, standard classification algorithms often exhibit a bias in predicting outcomes for the less represented classes [17,18]. The predominance of the majority class can substantially compromise the reliability of predictive models. This imbalance primarily manifests as inadequate performance in identifying cases from minority groups, which in turn adversely affects the efficiency of disease classification [19].

Chronic kidney disease (CKD) is one such medical condition characterized by heterogeneous and complex physiology. About 37 million US adults are estimated to have CKD, and most are undiagnosed. According to the Centers for Disease Control (CDC), it has been estimated that treating Medicare beneficiaries with CKD costs \$87.2 billion and treating people with end-stage renal disease (ESRD) costs an additional \$37.3 billion in 2019 [20]. Moreover, CKD has a global prevalence of over 10%, affecting over 800 million individuals [21]. During the past two decades, it has become one of the leading causes of death in the world as well as one of the few non-communicable diseases that has seen an increase in mortality rates [22]. The asymptomatic nature of CKD commonly delays diagnosis, often in more advanced stages, resulting in postponed implementation of prevention measures, diminishing patients' quality of life, and possibly irreversible kidney damage [23]. Consequently, the number of CKD patients requiring kidney dialysis has tripled over the last ten years [24]. Kidney dialysis is a medical treatment used to artificially filter and clean the blood; a function normally performed by healthy kidneys. It's typically used for individuals whose kidneys are no longer able to adequately remove waste products and excess fluid from the blood. In the US, nearly 808,000 people living with kidney failure need dialysis or a kidney transplant to survive (2 in every 1,000 people) [25]. However, not all patients with CKD undergo dialysis, leading to an imbalance in the CKD dataset [26]. This imbalance arises because the subset of CKD patients who require dialysis is significantly smaller compared to those who do not. Despite this, the ability to predict the need for dialysis in CKD patients is crucial. An early and accurate prediction can significantly impact patient outcomes,

allowing for timely interventions and better management of the disease. Hence, a decision support system capable of predicting the onset of dialysis, while effectively tackling the challenges of data imbalance, is crucial for enhancing the treatment and care of CKD. A clinical decision support system (CDSS) is a health information technology system designed to assist healthcare professionals by providing timely, relevant, and high-quality information, thereby improving the accuracy and efficiency of clinical decision-making. CDSS can range from simple alert systems to more advanced prediction frameworks incorporating complex ML algorithms and artificial intelligence (AI) [27]. A CDSS specifically designed for CKD patients can facilitate early detection of advanced stages and a need for dialysis [28]. The remarkable advancements in ML have revolutionized various aspects of healthcare, resulting in a rapid proliferation of ML-based CDSS which provide clinicians with evidence-based decision-making capabilities [29, 30]. It is largely due to its remarkable capabilities in diagnosis, prognosis, pattern recognition, and image classification, coupled with its remarkable processing speed and extensive analytic capabilities [31,32]. However, ML-based CDSSs remain limited in their deployment and broad adoption because of the inherent difficulties associated with implementing such models after incorporating the real-world complexities of patient care [33].

Despite significant advancements in CKD research, there is a lack of studies exploring the development of a ML-based CDSS for early dialysis prediction. One significant challenge for the development of ML-based CDSS arises primarily due to the inherent imbalance in datasets and the constraints imposed by the costs and time involved in acquiring additional information [34]. Generally, in electronic health record (EHR) data, it is difficult to extract an adequate sample of dialysis patients which poses a minority group problem, making the acquisition of sufficient samples impractical. This class imbalance problem has been addressed in a variety of ways over the past few years through the use of various data-driven approaches [35, 36]. Random sampling is the simplest and most popular method, in which objects are duplicated (oversampling) or removed (undersampling) randomly. However, it may result in the removal of patterns that can be useful for recognition or the duplication of non-valued samples [37]. By generating synthetic samples, more complicated techniques such as SMOTE (synthetic minority over-sampling technique) [38], ADASYN (an adaptive synthetic sampling approach) [39], and MWMOTE (Majority Weighted Minority Oversampling Technique) [40] attempt to reduce the impact of class imbalance. In addition, deep generative models such as GANs (Generative Adversarial Networks) [41,42] and statistical approaches such as copulas have also been used for synthetic data generation to address this problem [43,44]. While there are different methods for data augmentation and oversampling, these techniques have not been extensively developed for binary data. This limitation is particularly relevant in the healthcare sector, where binary data is prevalent [45,46]. Furthermore, it's vital to verify the distributional accuracy and feature similarity of these augmented samples, especially in the realm of medical datasets. This ensures that the augmented data accurately reflects the real-world patients with dialysis and maintains the integrity of the original dataset's characteristics.

Another significant challenge in developing an effective CDSS for dialysis prediction in CKD patients is choosing an appropriate evaluation metric that can accurately assess the performance of the underlying ML models. In scenarios with imbalanced data structures, a notable issue is the "accuracy paradox," where a model's accuracy may not truly represent its effectiveness [47]. For instance, a model might predict no future disease risk for all participants to achieve high accuracy,

which can be misleading [26]. Therefore, in medical applications, evaluation metrics like recall, precision, and the F1 score are more suitable for assessing the performance of ML models [48]. The choice of the primary metric depends on the specific application. Recall is particularly important as it measures the proportion of actual positive cases that the model correctly identifies, making it a vital metric for imbalanced data classification [49]. This is because, in imbalanced datasets, the minority class (which often represents the critical condition to predict, such as the need for dialysis in CKD patients) is more likely to be overlooked [50,51,52,53]. A model with high recall ensures that most of these critical cases are correctly identified, thereby enhancing the effectiveness and reliability of the CDSS in clinical settings.

In this study, we aim to address all the aforementioned challenges. The novel contributions of this study are summarized below:

- We develop a detailed data curation methodology that combines three extensive EHR data tables (Medication, Diagnosis, Procedure) related to CKD patients. This process focuses on accurately identifying patients who require dialysis, careful handling of missing values, organizing records based on clinical relevance, and employing expert-guided feature engineering to streamline the data. This meticulous preparation leads to the creation of a consolidated dataset for predicting the need for dialysis in advance. This refined dataset also serves as the foundation for applying ML models and further developing the CDSS.
- We propose a novel Binary Gaussian Copula Synthesis (BGCS) based augmentation method. The proposed BGCS method is specifically tailored to be used with binary data which is a characteristic of medical datasets.
- We evaluate the efficacy of various state-of-the-art (SOTA) data augmentation techniques, including our proposed BGCS method, to tackle the inherent data imbalance in the CKD dataset. Our approach includes both univariate and full feature space analysis, as well as the use of binomial proportion tests, to verify the distributional accuracy and statistical validity of the data augmented by these methods. The synthetic minority data produced by the BGCS method has been demonstrated to be more realistic and representative compared to other techniques, thereby making it a superior choice for data augmentation in this context.
- We also demonstrate how these synthetic samples generated by the augmentation methods improve the performance of ML models, with a particular emphasis on enhancing recall for the minority class, which is crucial in accurately predicting the need for dialysis in CKD patients at an early stage (i.e., 90 days ahead prediction before the identification of dialysis).
- Finally, we introduce a practical ML-based CDSS that utilizes a decision tree model. This choice is motivated by the interpretability of decision tree models in healthcare [54], which is crucial for presenting complex clinical data in a comprehensible way. The primary aim of the CDSS is to aid clinicians in making informed, evidence-based decisions about early dialysis prediction, ultimately enhancing patient care and outcomes.

The rest of the paper is organized as follows. Section 2 highlights recent literature in the area. The

CKD dataset used in this study and the steps followed to prepare the data are summarized in Section 3. Section 4 describes the preliminaries, definitions, and steps of our proposed method. Section 5 highlights computational results, and the comparative validation study of the different data augmentation and ML models. It also explains the CDSS introduced and developed in this study and discusses its findings. Finally, Section 6 provides concluding remarks and suggestions for future research.

2. Literature review

The purpose of this section is to analyze the literature comprehensively in two primary areas. The first step is to examine the imbalanced data challenge and the existing solutions used in healthcare. Following this, we examine recent advances in ML applications for CKD.

2.1. Imbalanced datasets in healthcare

As shown in Table 1, the research papers are summarized around several critical parameters, based on a concise summary of key aspects. The first step is to identify the specific disease addressed by each study, followed by the different types of data augmentation approaches employed in these studies. Additionally, the table highlights the diverse ML models used in different works. It also provides an overview of the types and characteristics of the data used in each study. A noteworthy feature of the table is that it indicates whether data generation has been analyzed in relation to model performance. Also, it reveals whether each paper has conducted a comprehensive feature analysis to quantify how the synthetically generated data matches the original ground truth. This includes univariate feature analysis, statistical analysis, and dimensionality reduction techniques (e.g., PCA (Principal Component Analysis) and tSNE (t-Distributed Stochastic Neighbor Embedding)) to analyze full space features.

Table 1: A summary of the healthcare research dealing with imbalanced data

Ref	Year	Disease	Data augmentation techniques	ML models	Data	Performance analysis	Full space feature analysis	Univariate feature analysis	Statistical analysis
[55]	2019	Complications post-bariatric surgery (including Diabetes, Angina, Heart Failure, and Stroke)	SMOTE, Random Under sampling, Ensemble Learning	Six popular classification methods	The Premier Healthcare Database (demographic and clinical attributes)	■	—	—	—
[56]	2019	Cerebral Stroke	PCA-Kmeans for pre-processing, Instance selection for under sampling	AutoHPO-based DNN	Health data from HealthData.gov used in a Kaggle competition	■	—	■	■
[57]	2020	General medical diagnosis	Misclassification-oriented Synthetic minority over-	Random Forest	Thyroid physical examination	■	—	—	■

			sampling technique (M-SMOTE) and Edited nearest neighbor (ENN)						
[58]	2021	Mechanically ventilated patients	SMOTE	XGBoost	Medical Information Mart for Intensive Care (MIMIC)-IV database	■	–	■	■
[59]	2022	End-Stage Kidney Disease (ESKD)	Synthetic Minority Over-Sampling Technique-Edited Nearest Neighbor (SMOTE-ENN)	Logistic regression analysis	A longitudinal database collecting electronic medical records of patients	■	–	–	■
[60]	2023	Trauma	SMOTE-based models	Six different classification methods	Trauma patient data from ICU	■	–	■	■
[61]	2023	HIV	GAN with VAE and external memory mechanism	downstream ML algorithms	Antiretroviral therapy for human immunodeficiency virus (ART for HIV).	■	–	■	■
[62]	2023	Chronic non-communicable diseases	SMOTE and ADASYN (ADaptive SYNthetic Sampling)	SVM, Random Forest, K-Nearest Neighbors, XGBoost	Eight medical datasets containing tabular data	■	–	■	■
[63]	2023	Sudden death in emergency department (ED) patients	K-means	logistic regression	emergency department data	■	–	■	■
[64]	2024	Not specific to one disease, but focuses on electronic health records (EHR) in general	Missing Value Imputation and Imbalanced Learning Generative Adversarial Network (MVIL-GAN)	MVIL-GAN, LightGBM	Tabular (EHR)	■	–	–	–
Our study	2024	Dialysis in CKD	SMOTE, GAN, Copula, BGCS	DT, RF, LR, and SVM	Real-world data (Binary Tabular)	■	■	■	■

In recent years, various approaches have been explored to address the challenge of imbalanced

data in medical datasets. Techniques like SMOTE and random under-sampling have been employed, with studies indicating a slight advantage of SMOTE over random under-sampling in enhancing model performance [55]. Hybrid ML approaches have been developed to tackle incomplete and imbalanced physiological data in clinical diagnosis, utilizing extensive medical records [56]. The integration of Modified Synthetic Minority Oversampling Technique (M-SMOTE) with Edited Nearest Neighbors (ENN) based on the Random Forest algorithm has shown promising results in outperforming other sampling algorithms across multiple datasets [57]. The application of SMOTE in developing ML models for predicting Methicillin-resistant *Staphylococcus aureus* (MRSA) in mechanically ventilated patients has also been explored, with synthetic datasets created to ensure balanced outcomes [58]. More recently, large datasets of individuals diagnosed with CKD have been analyzed, employing augmentation techniques like SMOTE-ENN and SMOTE-Tomek to address data imbalance [59]. Studies have also utilized SMOTE-based data pre-processing techniques in developing ML models for trauma datasets, demonstrating significant advantages of SMOTE-enhanced models over traditional methods [60]. The development of novel methodologies combining Variational Autoencoding (VAE) and Generative Adversarial Networks (GANs) has marked a significant advancement in generating synthetic datasets that accurately reflect imbalanced class distributions in clinical data analysis [61]. Efforts to enhance data balance have included the employment of different techniques to increase samples representing chronic non-communicable diseases. Evaluations of databases using synthetic data generation frameworks have been conducted, focusing on binary classification problems and chronic conditions [62]. The issue of significant imbalances in emergency department (ED) patient data has been addressed using models to identify risk factors for sudden death, employing algorithms like k-means [63]. A novel framework has been presented to tackle challenges associated with incomplete and imbalanced data in electronic health records (EHRs), combining missing value imputation with data generation and demonstrating its effectiveness using the MIMIC-IV dataset [64].

These studies collectively highlight the various models proposed to address data imbalance in healthcare. However, there is a gap in the literature regarding whether the synthetic data generation process accurately represents the actual data's underlying structures, particularly concerning techniques like PCA and t-SNE. Moreover, most studies have focused on a limited number of data generation methods. In contrast, the current study expands the range of methods examined, including a novel method specifically proposed for binary data, an important type of healthcare data. This emphasis on binary data, checking the statistical validity of the augmented data, and the comparative analysis of multiple augmentation methods represent a significant contribution to the field.

2.2. Recent advancements in the data-driven modeling approaches with CKD patients

In this section, we undertake an analysis of the recent advancements made in the data-driven decision frameworks involving CKD patients. Table 2 presents a comprehensive overview, categorizing each study based on several critical criteria: the specific focus within CKD research, the data challenges encountered, any strategies adopted to handle the data imbalance and whether the study has developed a CDSS or contributed to early prediction capabilities.

Table 2: A summary of the recent advancements in CKD research

Ref	Year	Focus	Data challenge	Balanced data checking	Number of augmentation models evaluated	CDSS	Early prediction
[65]	2023	Progression of urine protein	Missing data and imbalance	NO	1	■	■
[66]	2023	Predicting hyperkalemia	Missing values	Not applicable	Not applicable	–	–
[67]	2023	Predicting in-hospital mortality in ICU patients	Missing values, feature selection	Not applicable	Not applicable	–	■
[68]	2023	Analyze the complete blood cell count (CBC)-driven parameters	Small data size	NO	0	–	–
[69]	2023	Short timeframe (6–12 months) kidney failure risk prediction	Exclusion of some data because of missing values	Not applicable	Not applicable	–	–
[70]	2023	Analyze the performance of ML-based predictive risk models for CKD progression.	Selecting the candidates considering the availability of sufficient demographic data	Not applicable	Not applicable	–	■
[71]	2023	Identify clinical indicators	Considering the different input fields	Not applicable	Not applicable	–	–
[72]	2023	Early diagnosis and prediction of CKD progress	Missing values	Not applicable	Not applicable	–	■
[73]	2023	The identification of patients at risk of progressing to kidney failure	Missing values	Not applicable	Not applicable	–	–
[74]	2023	Identify different immune-related molecular clusters	Four raw datasets having duplicates	Not applicable	Not applicable	–	–
This study	2024	Identify the patients who need dialysis	Missing values, feature engineering, imbalanced data	Yes	4	■	■

In the realm of public health, CKD presents a significant challenge, necessitating the development

of predictive models for early intervention and appropriate resource allocation. The challenge of missing and imbalanced data in this context has been addressed in various studies, with one notable research focusing on the development of a CDSS [65]. This research utilized ML techniques to create an innovative framework for urine protein progression, involving a strategic selection of variables. A pool of 100 variables was narrowed down to 17 through a methodical recursive feature elimination procedure combined with logistic regression. The prediction of hyperkalemia in patients before their next clinic visit was the subject of a study employing a novel approach involving a human-machine competition [66]. This study, unique in its methodology, did not address the issue of data imbalance but found that the XGBoost ML model was more effective in predicting hyperkalemia in an outpatient clinic setting than nephrologists. Mortality rates in intensive care units, specifically among patients with CKD and coronary artery disease (CAD), were the focus of another study [67]. This research utilized the Boruta algorithm [75] for feature selection and demonstrated the efficacy of ML algorithms, particularly Gradient Boosting Decision Trees (GBDT), in predicting mortality rates. The handling of missing values was a critical component of this study, with variables having over 30% missing values being excluded and multiple imputations applied to the remaining data.

The analysis of parameters related to CKD based on complete blood cell count (CBC) in a cohort of pediatric patients was undertaken in a study by Kawalec et al. [68]. Despite acknowledging the limitation of a small dataset size, the study did not employ data generation techniques. It focused on a specific cohort of pediatric patients with stage 4 or 5 CKD and chronic dialysis patients, finding that CKD progresses into end-stage kidney disease (ESKD) as a result of chronic inflammation. Predicting kidney failure risk within a short timeframe for patients with advanced CKD was investigated in a study [69]. The study faced challenges due to the exclusion of certain data because of missing values. Despite these limitations, it emphasized the interpretability of its findings and demonstrated the superiority of ML models that incorporate time-updated data over traditional Cox regression models. A retrospective observational study using ML models based on random forest survival was conducted to assess CKD progression risk [70]. The study achieved high accuracy and an AUC of 0.85 for the progressive CKD risk classifier, although no CDSS was developed.

The potential of AI in predicting *Clostridioides difficile* infection (CDI) risk in a sample of CKD patients was explored in a study [71]. This research identified several risk factors for CDI development in CKD patients, including antibiotic use and emergency room stays prior to hospitalization. The identification of early signs of CKD and prediction of its progression was investigated by Liang et al. [72]. Despite not incorporating a CDSS, this research focused on early prediction using deep learning models combined with attribution algorithms (e.g. Integrated Gradients) [76]. 1000 CKD patients at risk of progressing to kidney failure were analyzed based on urinary peptidome in a study [73], which grouped patients into three distinct clusters with different CKD severities. Another study [74] conducted a cluster analysis using data from 440 CKD patients, employing weighted gene co-expression network analysis to identify core immune-related genes (IRGs), leading to the identification of two distinct subtypes of CKD characterized by different patterns of immune gene expression.

To date, most of these studies have not taken into consideration the development of a CDSS, an important component of enhancing interpretability and facilitating an easier understanding of

clinical data. It is also noteworthy that early prediction has been underexplored in these studies in the context of CKD. In addition, many studies failed to adequately deal with data imbalance, relying on datasets accumulated over extended periods [44,45,56,57,58]. By addressing issues related to missing values, handling a large number of features, and data imbalance, our study attempts to address these gaps. In addition, we emphasize the development of a CDSS and the integration of early prediction mechanisms.

3. Data Understanding

This study utilized an EHR dataset collected from TriNetX, a global network platform that facilitates data gathering and utilization by healthcare institutions worldwide. To maintain accuracy and adhere to a standardized format, TriNetX retrieves patient data from EHR across different healthcare organizations (HCOs). Data on the platform can be categorized into demographics, diagnoses, procedures, lab results, medications, and vital signs. Utilizing the rich and standardized data available through TriNetX, this study focused on patients with CKD from West Virginia (WV), USA. A single-center, retrospective observational study is conducted in accordance with STROBE guidelines [77]. This study involves 90,602 patients whose medical records covered the period from February 2008 to June 2022. We employ the International Classification of Diseases, 10th Revision, Clinical Modification (ICD-10-CM) coding system to pinpoint the initial CKD diagnosis date. Specifically, we have filtered the diagnosis file for entries commencing with the "N18" code, which denotes CKD cases [78]. This study focuses on patients who had acute kidney injury (AKI) within 90-days of any inpatient hospitalization. Among hospitalized patients and critically ill adults, AKI is extremely prevalent and has diverse complications. It is estimated that 15% of hospitalized patients and 60% among critically ill adults are diagnosed with AKI, respectively [79]. Diagnosis, procedures, and medications are recognized as being significant factors associated with CKD and AKI [80,81,82]. Based on the ICD-10-CM procedure codes "90935", "90937", "90945", "90947", and ICD-10-CM diagnosis codes "Z99.2", dialysis patients were identified in the corresponding datasets.

To maintain the focus of our analysis on the progression leading to dialysis initiation in CKD patients, we exclude cases where dialysis occurred before CKD. To emphasize the importance of early prediction, only the first dialysis event following the diagnosis of CKD for each patient is considered, thereby preventing the influence of subsequent treatments. Our analysis has focused on diagnoses made before the initial dialysis event in CKD patients to provide a comprehensive understanding of the pre-dialysis phase. Furthermore, we have included only procedures and medications administered after CKD diagnosis and before the first dialysis is scheduled. Through this approach, we could concentrate exclusively on treatments and interventions that occurred between the diagnosis of CKD and the dialysis initiation. This dataset encompasses 459,868 records, representing 15,169 unique CKD patients. The process of obtaining the study dataset by using the main database is illustrated in Figure 1. Based on Figure 1, the following steps are required to prepare the data used for this study after the described steps. The key factors in preparing the data are as follows:

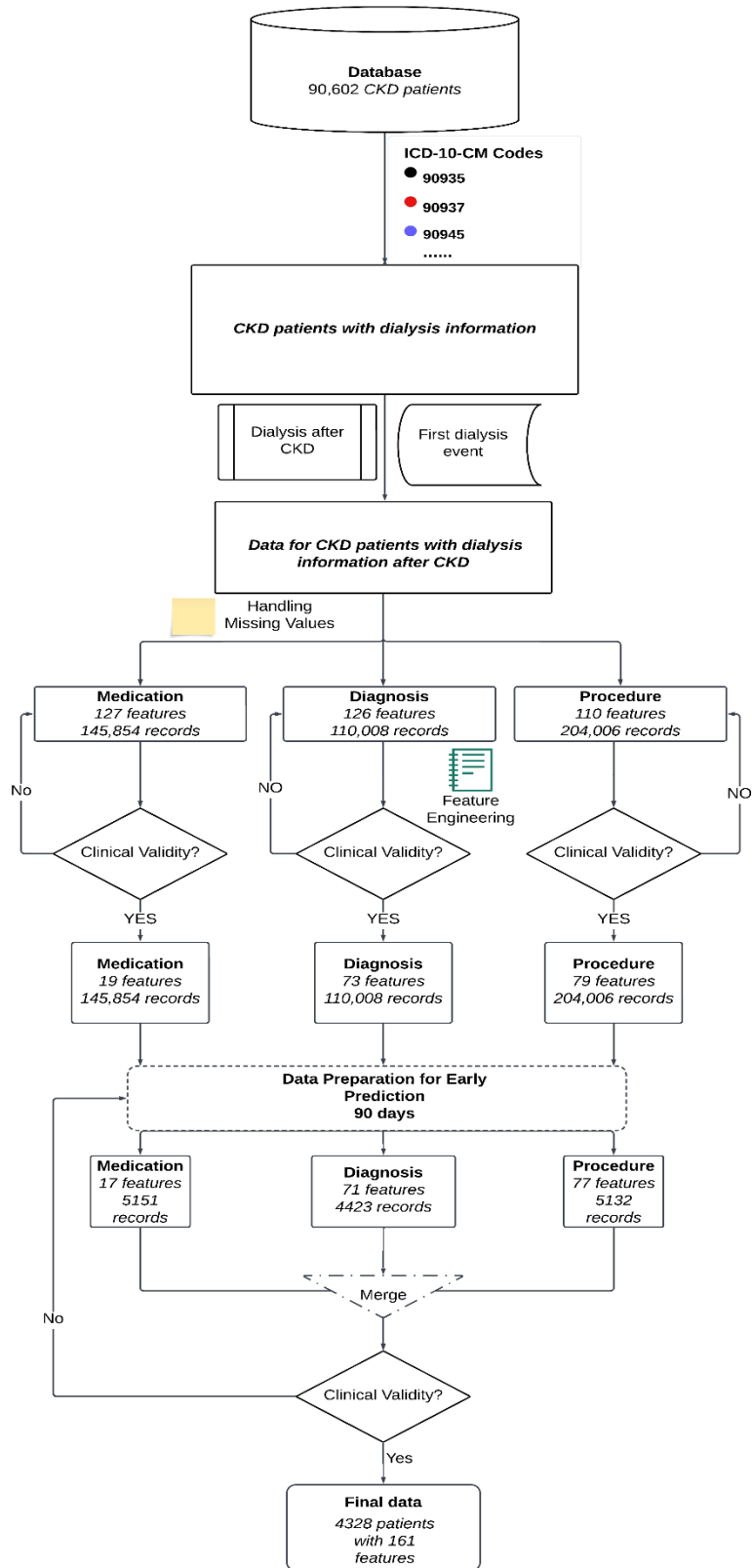


Figure 1: An illustration of the study design schema depicting the process of obtaining study data

- Missing Values and Feature Engineering:** Guided by medical experts, some observations are completed, ensuring no bias or distortion is introduced into the data. Some observations are omitted to maintain data integrity, particularly in cases where imputation could compromise accuracy or introduce uncertainty. For binary variables like medication use and comorbidities, missing values are assigned zeros to signify absence or non-use [78]. Our analysis integrates three distinct data sources: Medication, Procedure, and Diagnosis. The Medication dataset, with 145,854 entries, details all medications given to patients. The Procedure dataset, comprising 204,006 records, logs each patient's medical procedures. The diagnosis dataset, containing 110,008 entries, records patient comorbidities. Feature engineering, guided by medical experts, is pivotal in refining these datasets for more effective analysis. Initially, the Medication dataset had 123 binary features, which were streamlined to 15, grouping similar medications and focusing on the most impactful ones. This has not only made the data more manageable but also enhanced the precision of our predictions, ensuring clinically relevant classifications. The Procedure and Diagnosis datasets has gone through a similar refinement, with the number of features in Procedures reduced from 106 to 75 and in Diagnosis from 122 to 69. Reducing the number of features is crucial as it directly influences the quality and performance of our ML models, ensuring they are both efficient and clinically applicable.

Table 3: Summary of the Datasets Refinement in CKD Patient Data

<i>Attribute</i> \ <i>Dataset</i>	Medication	Diagnosis	Procedure
Observations	145,854	110,008	204,006
Features (Before feature engineering)	127	126	110
Binary Features (Before feature engineering)	123	122	106
Binary Features (After feature engineering)	15	69	75
Patients	4561	5295	5313
Records per patient (Range)	(1,117)	(1,114)	(1,106)
Records per patient (Median)	30	18	37
Records per patient (Average)	~32	~21	~38
CKD date	02/2008-04/2022	02/2008-04/2022	02/2008-04/2022

As shown in Table 3, the datasets include information from 4561, 5313, and 5295 patients respectively, reflecting the difference in nature and requirements of these datasets. The range of records per patient provides insight into the dataset's depth, with the Medication dataset ranging from 1 to 117 records per patient, the 'procedure' dataset ranging from 1 to 106, and the 'diagnosis' dataset ranging from 1 to 114 records per patient. Each dataset contains approximately 30 records per patient in Medication, 37 records in Procedure, and 18 records in Diagnosis, thus providing further insight into the typical patient profile. A longitudinal perspective is utilized to understand the dialysis need for CKD patients covering from February 2008 to April 2022.

- Data Preparation for Early Prediction:** The data preparation involved a crucial step in calculating the duration between the initiation of dialysis and the initial diagnosis of CKD. Our data set is modified to include this added feature, which is computed in days. To align with early prediction, we filter this dataset based on the newly calculated duration. Specifically, we examine cases where the interval between diagnosis of CKD and initiation of dialysis is at least 90 days. Then to accurately reflect the early prediction scenario (90 days ahead prediction), we delete any record for the dialysis patients within 90 days of their dialysis. Next, date information is converted into a standardized time format, which enables the data to be sorted chronologically. For subsequent analyses to accurately account for the temporal aspects of patient treatment histories, this step is crucial. To prioritize the most recent records, the data is sorted according to patient identifiers and dates after the date conversion. The latest data often holds the most relevance for clinical decision-making and outcome prediction, so this sorting is crucial for prioritizing recent patient interactions with the healthcare system. Our data refinement process includes filtering the records in such a way that only the first occurrence of each unique medication class per patient would be retained. Thus, we reduce the redundancy of the data by eliminating repetitive entries of the same medication class for individual patients. This process has been repeated for all three datasets (Medication, Diagnosis, and procedure). Then, the three datasets are merged to create a unified dataset that represents the complexity of patient information. Using the *'patient_id'* column, a common identifier across all three datasets, the merge process is conducted. As a result, the records are accurately consolidated for each patient, ensuring that their medical histories remain intact. As a result, only patients identified in all three datasets are included in the final merged dataset (4328 patients with 161 features). The overall process to reach the final dataset is shown in Figure 2.

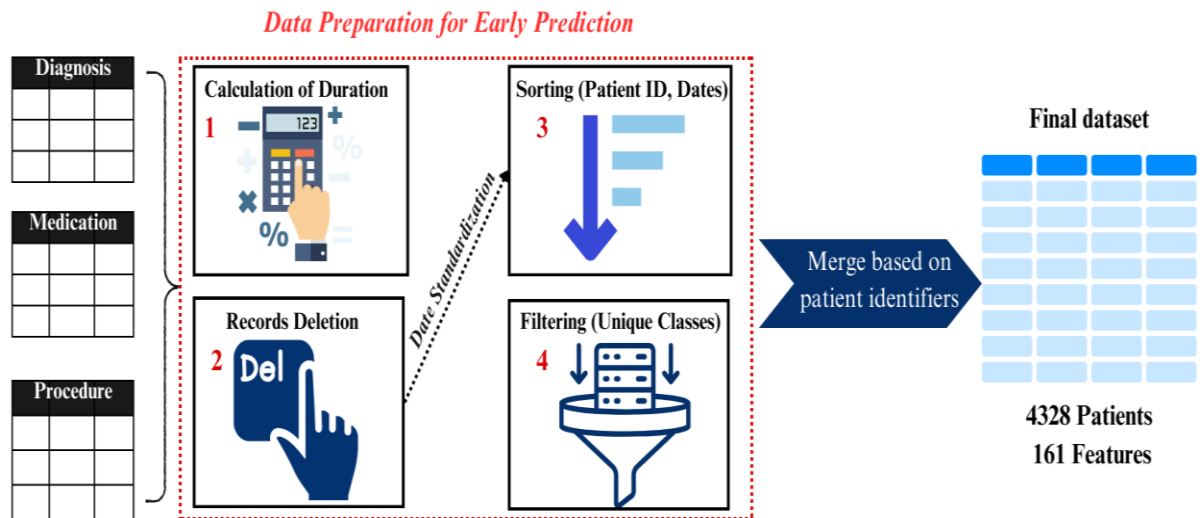


Figure 2: Data preparation workflow for early prediction analysis

In the final dataset used for this study (see **Appendix A**), there are significant challenges associated with the imbalanced nature of the data, with approximately 5% of the data representing class 1. The imbalance significantly impacts the performance of predictive models, particularly the ability to predict the need for dialysis. For example, when using the Random Forest model on this dataset,

class 1 has a limited recall of 45%. This imbalance is clearly illustrated in Figure 3 below, which visualizes the distribution of classes within the dataset.

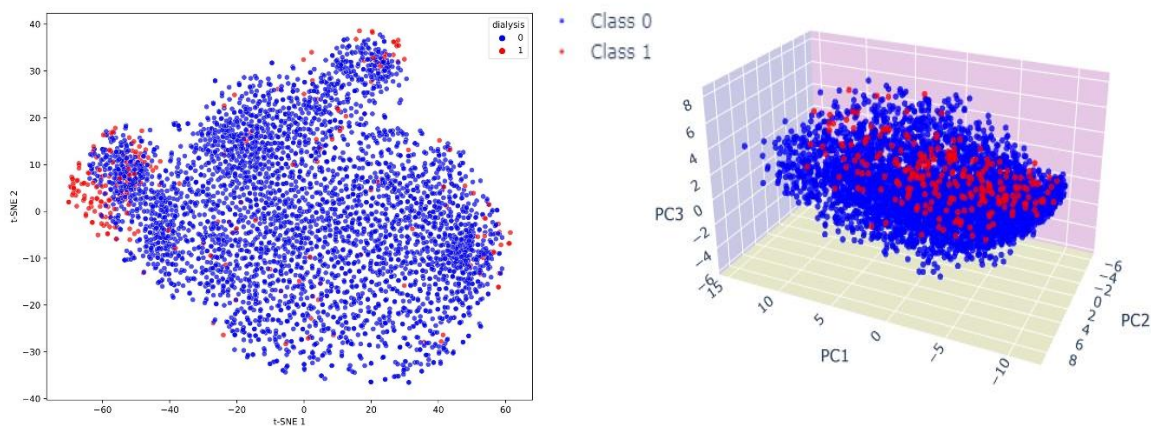


Figure 3: Visualization of the dataset's imbalance utilizing dimensionality reduction techniques, t-SNE and PCA

Considering two dimensionality reduction techniques, t-SNE and PCA, Figure 3 illustrates the imbalance in the dataset, respectively by converting the high-dimensional data into two and three dimensions. The t-SNE plot demonstrates the disparity in the distributions between the two classes by color-coding the data points. The PCA plot, similarly, illustrates the spatial relationship between the classes.

4. Methodology

In this section, we initially outline the performance metrics used in our analysis. Following this, we detail various data augmentation techniques, including a step-by-step explanation of our proposed BGCS method.

4.1. Performance Assessment

Confusion matrices are fundamental tools in ML and statistics, and they are primarily used to evaluate the performance of classification models, particularly binary classification models. Typically, the matrix tabulates the number of samples for each combination of the reference class and predicted class to provide a comprehensive summary of the model's predictions as compared to actual true outcomes. It is common practice to designate a binary confusion matrix as a positive-negative matrix, in which the class of interest is designated as a positive class, while the background class is designated as a negative class (Table 4). A binary classification is characterized by four possible outcomes: true positives (TPs) and true negatives (TNs). True positives indicate the accurate classification of positives and negatives. False positives (FPs) result from the incorrect classification of background classes as positive classes, whereas false negatives (FNs) result from the incorrect assignment of positive classes to background classes [83].

Table 4: The confusion matrix for binary classification. TP = True Positive, TN = True Negative, FP = False Positive, and FN = False Negative.

		Reference Data	
		Positive	Negative
Classification Result	Positive	TP	FP
	Negative	FN	TN

Several metrics can be calculated from this cross-tabulation, including precision (as shown in Equation (1)), which indicates how many samples are correctly classified among those that are predicted to be positive. Recall (as defined in Equation (2)) indicates the proportion of instances correctly classified within the positive class to those in the reference data. Equation (3) represents the ratio of correct samples (both positives and negatives) to the total number of samples known as accuracy [84].

$$Precision = \frac{TP}{TP+FP} \quad (1)$$

$$Recall = \frac{TP}{TP+FN} \quad (2)$$

$$Overall Accuracy = \frac{TP+TN}{TP+TN+FP+FN} \quad (3)$$

Considering the aim of the study, which is early prediction of the dialysis, recall metric is considered as the main focus of the paper.

4.2. CTGAN

Conditional Tabular Generative Adversarial Network (CTGAN) is a generative model designed specifically to generate tabular data that maintains the statistical characteristics of the source data while enabling the creation of data under specific conditions [85]. Data presented in tabular form, which are rows and columns organized in a grid format similar to spreadsheets or databases, provide the basis for the analysis. The CTGAN method uses a GAN-based method to model tabular data distributions and generate synthetic rows based on those distributions. Using a conditional generator, the CTGAN employs a training-by-sampling strategy to deal with the issues associated with non-Gaussian and multimodal distributions. As part of its architecture, several new techniques are integrated into the model to provide high-quality results. CTGAN uses specific conditions to enhance the data generation process while maintaining the fundamental learning approach used in GANs [86,87]. CTGAN leverages two neural networks – a generator (G) and a discriminator (D) – in a competitive training paradigm. G seeks to generate data mimicking real samples, while D strives to differentiate between real and synthetic data. This adversarial interaction progressively enhances G 's capability to generate increasingly realistic data. Here is the equation representing the objective function of this approach.

$$\min_G \max_D V(D, G) = E_{x \sim p_{data}(x)} [\log D(x|y)] + E_{z \sim p_z(z)} \left[\log \left(1 - D(G(z|y)) \right) \right] \quad (4)$$

where $p_{data}(x)$ indicates original data and $p_z(z)$ represents the synthetic data. The discriminator,

D , accepts real data input donated as x and assesses its authenticity, yielding a probability score, $D(x)$. The generator, G , utilizes a random noise vector z to synthesize artificial data shown by $G(z)$. The discriminator's goal is to accurately classify real data, aiming for $D(x)$ to approach 1, while assigning a probability of 0 to synthetic samples, $D(G(z|y))$. Conversely, G 's objective is to generate data so convincing that $D(G(z|y))$ approaches 1, effectively tricking D . This establishes a dual optimization dynamic, as the discriminator aims to maximize its accuracy, while the generator attempts to minimize D 's ability to differentiate [86]. The overall framework of this method can be seen in Figure 4.

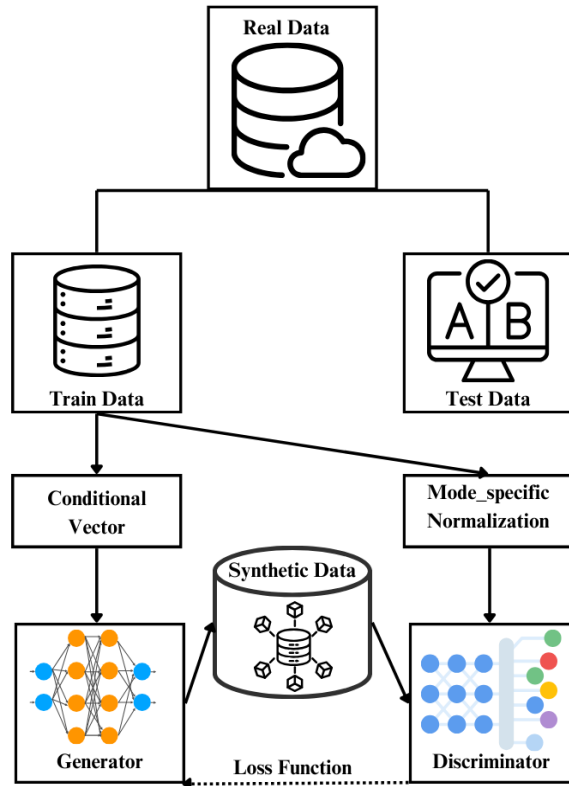


Figure 4: Overall framework of CTGAN to generate synthetic data.

It should be noted that the novel synthetic samples generated by CTGAN do not replicate the instances in the original dataset but rather closely resemble them [88]. Considering the performance of this algorithm, it can be used in a variety of data science and ML applications, particularly data generation to deal with imbalanced datasets.

4.3. SMOTE

SMOTE is a popular algorithm that has been employed to address the issue of class imbalance in the ML domain. By generating synthetic data for the minority class, SMOTE is a method for addressing class imbalance through oversampling. It prevents overfitting when using random oversampling [89]. By connecting data points to their k -nearest neighbors, SMOTE generates new data points for the minority class. There is an important distinction between the synthetic data points created through SMOTE and the minority class instances. According to [90], it is essential to distinguish between these two points so that overfitting can be avoided during model training.

The steps of this method can be summarized as follows [38]:

4.3.1. Sample Identification of Minorities: First, the dataset is analyzed to select samples belonging to the minority class. The purpose of this step is to ensure that the oversampling process is focused only on the underrepresented group.

4.3.2. Nearest Neighbor Calculation: A minority sample is determined to have 'k' nearest neighbors within the same class. The neighbors of the k nearest neighbors are randomly selected depending on the amount of over-sampling required.

4.3.3. Analyses of Oversampling Rates: Oversampling should be expressed as a percentage, as this determines how many synthetic samples are required. A 200% oversampling rate, for example, would result in two additional synthetic samples being generated for each minority class sample.

4.3.4. Random Selection: A random subset of the nearest neighbors for each minority class sample is selected according to the oversampling rate. For example, in the case of a 200% oversampling rate, two neighbors would be selected randomly from k neighbors.

4.3.5. Synthetic Data Generation: Steps to be performed for each selected nearest neighbor of a minority class sample are as follows:

- The vector difference between the sample feature vector and its nearest neighbor from the minority class is calculated.
- The difference between these two vectors is multiplied by a random number uniformly distributed between 0 and 1.
- When the scaled difference between the original sample and its neighbor is added to the original sample of the minority class, a synthetic sample is created by randomly choosing a point along the line segment between the original sample and its neighbor.

The aforementioned process should be repeated for each minority class sample until the oversampling requirement is met.

4.4. Gaussian Copula

A copula is a powerful tool for capturing and replicating the dependency structure of multivariate distributions in the field of synthetic data generation. Sklar's theorem [92], states that any multivariate joint distribution can be expressed in terms of its univariate marginal distributions and a copula C which captures the dependency between the variables. The theorem states that the probability density function (PDF) of X can be written as:

$$p(x_1, \dots, x_n) = c(F_1(x_1), \dots, F_n(x_n))p_1(x_1) \dots p_n(x_n) \quad (5)$$

where $p_j(x_j)$ is the PDF of X_j , corresponding marginal cumulative distributions (CDF) F_1, \dots, F_n , and c is the copula density. For multivariate data, this provides the ability to separately capture marginal distributions and their dependency structure and as a result, it is possible to model complicated relationships between variables. The multivariate cumulative distribution F for n random variables z_1, \dots, z_n with F_1, \dots, F_n is expressed as follows [93]:

$$F(z_1, \dots, z_n) = C(F_1(z_1), \dots, F_n(z_n)) \quad (6)$$

Based on this equation, the copula C can be used to determine the joint distribution, representing the relationship between variables once the appropriate marginal distributions have been estimated. To employ copulas, first, the marginal cumulative distribution functions $\hat{F}_1, \dots, \hat{F}_n$ are

derived to construct pseudo-observations $\hat{U}_1 = \hat{F}_1(Z_1), \dots, \hat{U}_n = \hat{F}_n(Z_n)$. The pseudo-observations are uniformly distributed by definition and serve as inputs to the copula which also contains the dependence structure of the data. Synthetic samples are generated by simulating uniform random variables U_1, \dots, U_n from the estimated copula C and these marginals. Finally, a synthetic dataset is created by inversely transforming these uniform variables into the original space of data based on equation (7) [93]:

$$Z_1 = \hat{F}_1^{-1}(X_1), \dots, Z_n = \hat{F}_n^{-1}(X_n) \quad (7)$$

Gaussian Copulas, which are derived from multivariate normal distributions, are particularly useful when the variables exhibit linear relationships between them. The n -variate Gaussian copula C is expressed as [94]:

$$C^n(\mathbf{u}) = \Phi_{\Sigma}^n(\Phi^{-1}(u_1), \dots, \Phi^{-1}(u_n)) \quad (8)$$

where Φ_{Σ}^n is the joint CDF of the n -variate normal distribution with a linear correlation matrix Σ , Φ^{-1} is the inverse CDF of the univariate standard normal distribution, and \mathbf{u} is a vector of univariate uniformly distributed values. Based on equation (6) above, the joint CDF of a pair of binary variables Y_1 and Y_2 using a copula C is given by $F(y_1, y_2) = C(F_1(y_1), F_2(y_2))$, where F_1 and F_2 are the CDFs of the univariate binary distributions. The joint probability mass function (PMF) can be recovered from the CDF using the relation [95]:

$$P(Y_1 = y_1, Y_2 = y_2) = C(F_1(y_1), F_2(y_2)) - C(F_1(y_1 - 1), F_2(y_2)) - C(F_1(y_1), F_2(y_2 - 1)) + C(F_1(y_1 - 1), F_2(y_2 - 1)) \quad (9)$$

Setting y_i to 0 or 1 and noting that $F_i(0) = P(Y_i = 0) = 1 - p_i = q_i$, based on the equation, probabilities can be calculated for each configuration of binary outcomes. When employing the Gaussian copula C_1 with the parameter $\theta = \gamma$, representing the correlation coefficient, the correlation between Y_1 and Y_2 , denoted by ρ , can be obtained by solving [95]:

$$\rho = \text{Corr}(Y_1, Y_2) = \frac{C_1(p_1, p_2; \gamma) - \sqrt{p_1 p_2}}{\sqrt{p_1 q_1 p_2 q_2}} \quad (10)$$

In summary, the Gaussian Copula, a statistical model, generates synthetic data with an estimated correlation matrix. This model transforms marginal distributions to a uniform distribution, then applies the Copula to create correlated uniform variables, and finally transforms back to the original space using inverse CDF. The overall process of this method Copula is shown in Figure 5.

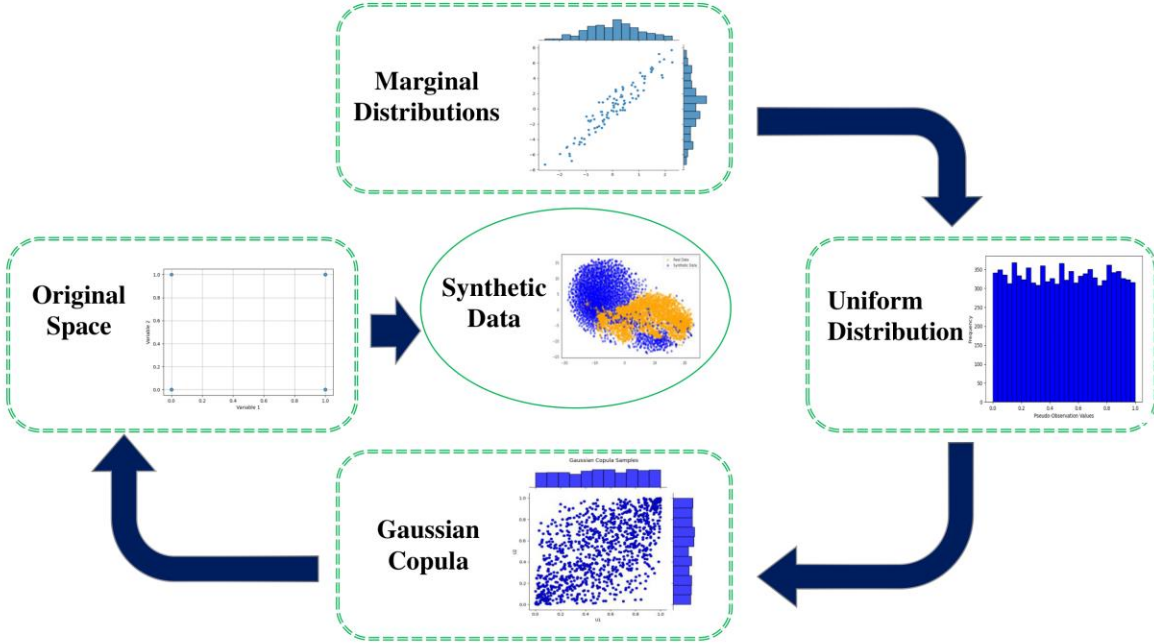


Figure 5: Overall framework of Gaussian Copula to generate synthetic data

4.5. Binary Gaussian Copula Synthesis

While methods like SMOTE, CTGAN, and Copula are effective for creating synthetic data, they aren't tailored for binary data generation. Considering the prevalence of binary data in numerous fields, particularly in medical datasets, there is a significant need for a method adept at handling binary datasets. In response to this, we have developed the Binary Gaussian Copula Synthesis (BGCS) method, inspired by the Gaussian Copula approach. BGCS is specifically designed to generate synthetic data that accurately reflects real-world binary data, with the potential to significantly enhance the performance of ML algorithms. This subsection will provide a detailed, step-by-step explanation of the augmentation mechanism employed in our BGCS method.

Let \mathcal{C} be a Gaussian copula with a correlation matrix Σ of size $n \times n$, where n is the number of variables. The copula is defined as follows [95]:

$$\mathcal{C}(u_1, u_2, \dots, u_n) = \Phi_n(\Phi^{-1}(u_1), \Phi^{-1}(u_2), \dots, \Phi^{-1}(u_n); \Sigma) \quad (11)$$

where:

- Φ_n is the cumulative distribution function (CDF) of the multivariate normal distribution with mean vector $\mathbf{0}$ and correlation matrix Σ .
- Φ^{-1} is the quantile function (inverse CDF) of the univariate standard normal distribution.
- u_1, u_2, \dots, u_{12} are the uniform marginals obtained from the original data's empirical CDFs.

Calculating a correlation matrix Σ used in the multivariate normal sampling, which is crucial in capturing the dependency structure inherent in the data, defined as:

$$\Sigma = \begin{bmatrix} 1 & \rho_{1,2} & \cdots & \rho_{1,n} \\ \rho_{2,1} & 1 & \cdots & \rho_{2,n} \\ \vdots & \vdots & \ddots & \vdots \\ \rho_{n,1} & \rho_{n,2} & \cdots & 1 \end{bmatrix} \quad (12)$$

where $\rho_{i,j}$ is the correlation coefficient between the i -th and j -th variables ($\rho_{i,j} = \rho_{j,i}$). The procedure for generating synthetic data using Binary Gaussian Copula Synthesis, as a binary variant of Gaussian Copula, is as follows:

4.5.1. Sample Generation:

For an n -dimensional binary data vector where n is the number of features, we begin by sampling from a multivariate normal distribution with zero mean and a given correlation matrix $\Sigma \in \mathbb{R}^{n \times n}$ which is derived from the available data. Each vector sample $\mathbf{z} \in \mathbb{R}^n$ is generated as:

$$\mathbf{z} \sim \{\mathbf{x}_1, \mathbf{x}_2, \dots, \mathbf{x}_m\} \propto \mathcal{N}(\mathbf{0}, \Sigma) \quad (13)$$

where $\mathbf{0}$ is an n -dimensional zero vector and $\mathbf{x}_i \in \mathbb{R}^n$ for $i = 1, 2, \dots, m$. A desired number of samples is denoted as m .

4.5.2. Transformation to Uniform:

Each component z_i of the vector sample \mathbf{z} is transformed into a uniform marginal using the cumulative distribution function (CDF) of the standard normal distribution, Φ :

$$u_i = \Phi(z_i) = (\Phi(x_{i1}), \Phi(x_{i2}), \dots, \Phi(x_{in})), \quad i = 1, \dots, n \quad (14)$$

The resulting vector $\mathbf{u} = (u_1, \dots, u_n)$ follows a uniform distribution on the interval $[0,1]$ and $\mathbf{u}_i \in [0,1]^n$.

4.5.3. Binary Conversion:

Each element u_{ij} of \mathbf{u} is compared to the corresponding marginal probability p_j , which is used as a threshold to convert the uniform variables into binary outcomes. The marginal probability p_j for each feature j is the empirical probability that the variable takes on the value 1 in the original dataset. It can be calculated as the mean of the feature across all records. Here's the mathematical formulation for p_j :

$$p_j = \frac{1}{l} \sum_{i=1}^l X_{ij} \quad (15)$$

where:

- l is the total number of records in the original dataset,
- X_{ij} is the value of the j -th feature in the i -th record of the original dataset
- $X_{ij} \in \{0,1\}$ for binary features.

Given a vector of marginal probabilities $\mathbf{p} = (p_1, \dots, p_n)$, the uniform marginal is transferred to binary outcomes. For each element u_i of vector \mathbf{u} , the binary data vector \mathbf{b} is calculated by:

$$b_i = \begin{cases} 1 & \text{if } u_i < p_i \\ 0 & \text{otherwise} \end{cases} \quad (16)$$

Which leads generating the synthetic binary data:

$$\mathbf{S} = \{\mathbf{s}_1, \mathbf{s}_2, \dots, \mathbf{s}_m\} \quad (17)$$

where $s_i = (I(u_{i1} < p_1), I(u_{i2} < p_2), \dots, I(u_{in} < p_n))$ and I is the indicator function, such that $I(\text{condition}) = 1$ if the condition is true and 0 otherwise. In matrix notation, the transformation from multivariate normal samples to synthetic binary data can be represented as:

$$\mathbf{S} = 1\{\Phi(\mathbf{X}) < \mathbf{p}\} \quad (18)$$

4.5.4. Synthetic Data Generation:

Repeating the above process m times yields m synthetic binary vectors, constructing a synthetic dataset $\mathbf{B} = \{\mathbf{b}_1, \mathbf{b}_2, \dots, \mathbf{b}_m\}$. In this process, to ensure that the transformed marginals are uniformly distributed, the CDF of the standard normal distribution is used to transform the multivariate normal samples into uniform marginals. Setting a threshold based on marginal probabilities ensures that the synthetic data matches the marginal probabilities: $\forall i, P(b_i = 1) = P(u_i < p_i) = p_i$, which is because for a uniform random variable U we have $P(U < k) = k$ for any $k \in [0,1]$. Also, using the Gaussian copula model, the Gaussian correlation matrix captures the dependence structure defined by Σ . Since the transformation to uniform marginals is monotonic, the rank order is preserved and the correlation in the synthetic data $\rho_{i,j}^{syn}$ is defined as follows:

$$\forall i \neq j, \rho_{i,j}^{syn} \approx \rho(\Phi^{-1}(u_i), \Phi^{-1}(u_j)) \approx \rho_{i,j} \quad (19)$$

where ρ denotes the Pearson correlation coefficient, and $\rho_{i,j}$ is the correlation coefficient specified in Σ . So, for features i and j , the correlation in the synthetic data $\rho_{i,j}^{sym}$ approximates the correlation in the original data $\rho_{i,j}^{orig}$:

$$\rho_{i,j}^{syn} \approx \rho_{i,j}^{orig} \quad (20)$$

With the help of this process, we can generate a synthetic binary dataset that approximates the correlation structure observed in the original data while adhering to the predetermined marginal probabilities and maintaining the correlation structure in the original data. By using the Gaussian copula's properties to model the correlation between binary features, this method creates a dataset that reflects real-world interdependencies.

5. Results and Discussion

This section begins with an assessment of the effectiveness of the data augmentation techniques and performance analysis of the ML models after augmentation. Then, the development of the proposed CDSS is explained. In the first part, we initially analyze the distribution of individual

features to evaluate the efficacy of various data augmentation methods. Following this, we assess the statistical validity of the augmented data by comparing its features to those of the original data using a binomial proportion test. Then, a thorough comparison of the structural differences between synthetic and real data is conducted, utilizing dimensionality reduction techniques. Furthermore, we examine how the synthetic samples, generated by these different methods, impact the performance of ML models. In the second part, early prediction of dialysis is prioritized to develop the CDSS, and its steps are explained. The process begins with data preparation and leads to the establishment of decision-making rules, ultimately assisting clinicians in making more informed decisions.

5.1. Augmentation validity and performance analysis

This subsection evaluates the reliability of synthetic data produced by various techniques. Initially, we analyze a selection of representative features from the dataset individually, using cumulative sum (cumsum) and probability distribution plots. This will be followed by a statistical analysis to gauge the similarity between the synthetic (fake) and real data. Lastly, we assess the entire feature space through techniques like PCA and t-SNE to understand the overall data structure and integrity.

5.1.1. Univariate feature analysis

All the features start with a letter from the alphabet according to their medical category. ICD-10-CM categorizes similar features (i.e., infectious disease, respiratory disease, etc.) with similar letter codes. We choose a representative feature for each group of letter codes. The selection of this feature is based on frequency of occurrence, clinical significance, data quality and completeness, and diversity and uniqueness to ensure that it reflects the overall characteristics of its group. The application of this method allows us to analyze each feature group in a focused manner by examining the representative of each group. Figures 6 to 8 illustrate three different types of visual comparison based on the selected features from these groups.

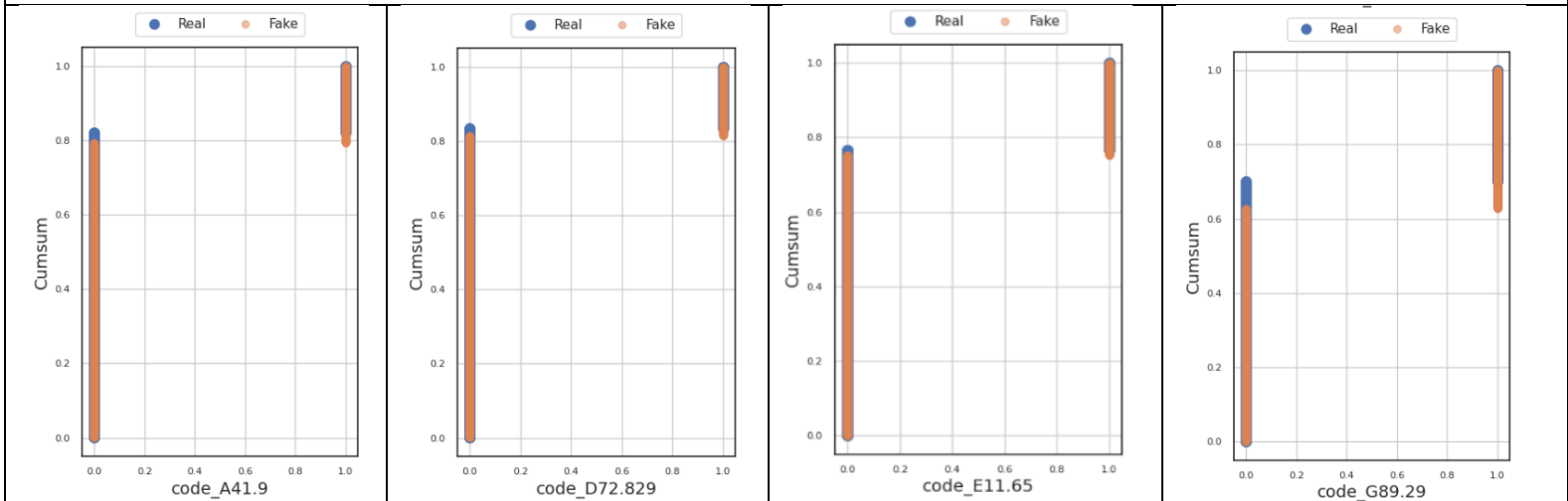
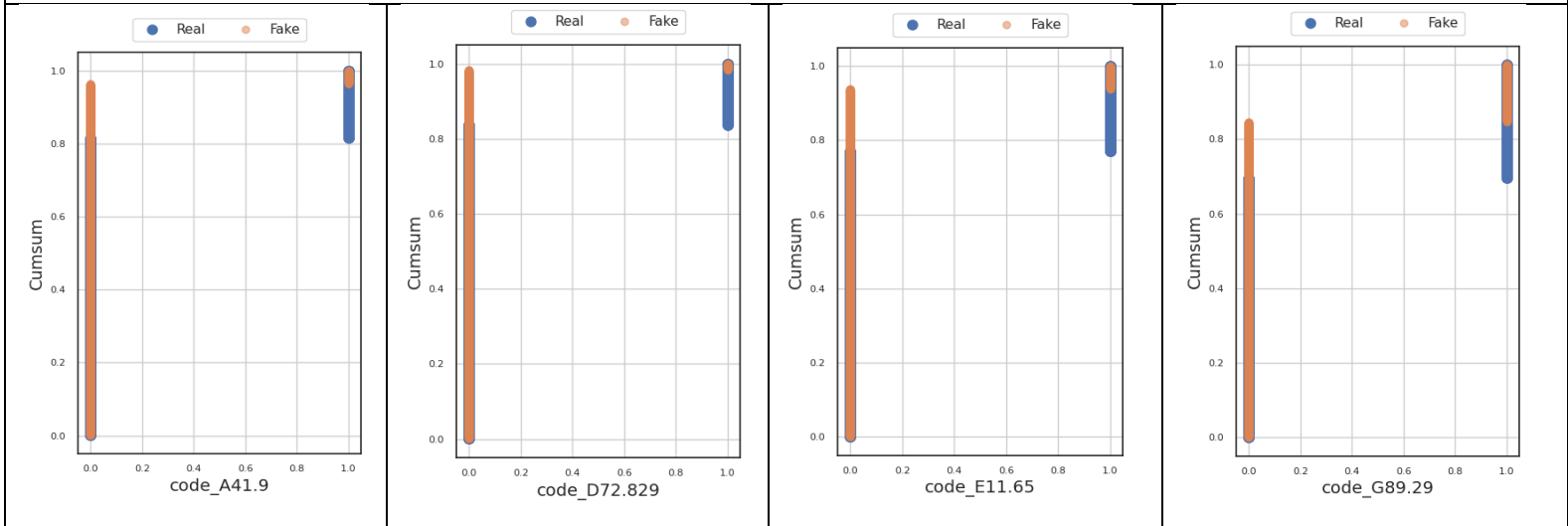
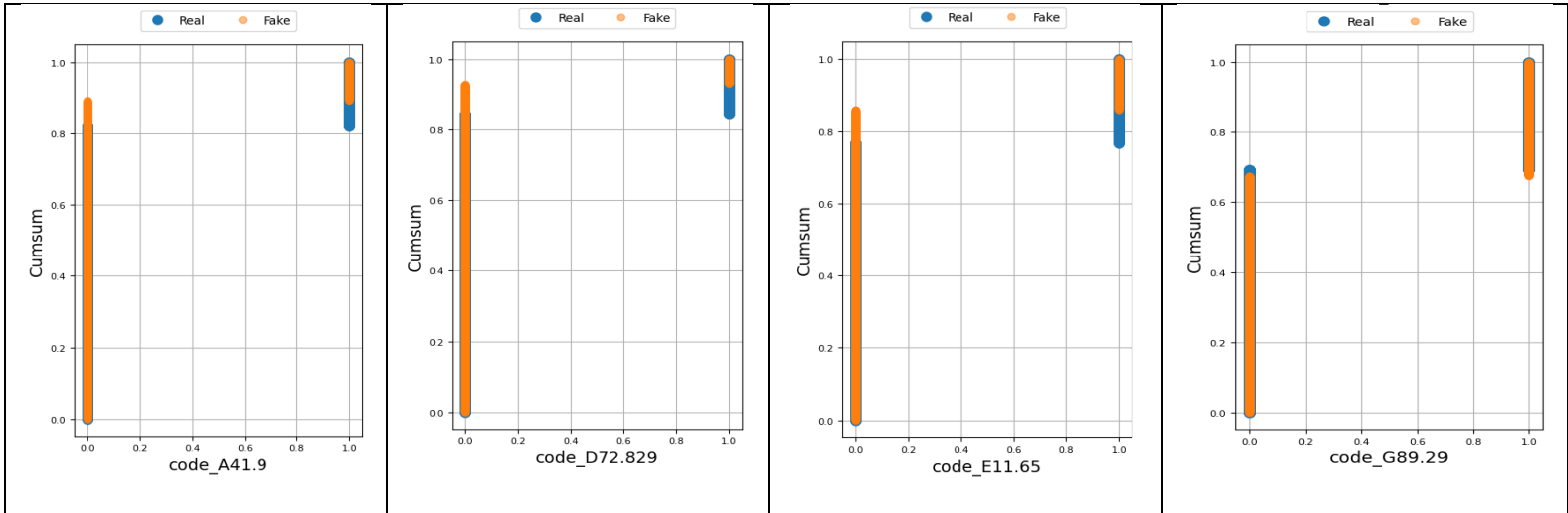
Figure 6 presents a cumsum plot that illustrates the cumulative distribution of feature set 1 including codes A41.9¹, D72.829², E11.65³, and G89.29⁴ for both real (blue) and synthetic data (orange). On this plot, the y-axis shows the cumulative proportion of samples, while the x-axis displays the range of values. For the data augmentation techniques to be deemed effective, there should be a notable overlap between the real and synthetic data lines. Essentially, the synthetic data should closely mirror the real data across the entire value range, with minimal divergence between the two. As indicated in the figure, the Gaussian Copula and BGCS methods are particularly adept at creating synthetic data that aligns well with the real data distribution across various feature groups. Upon closer inspection, BGCS shows marginally superior performance, especially in replicating the full distribution of the second and third features with high accuracy. While SMOTE and CTGAN are also useful, they tend to yield more scattered distributions that don't consistently reflect the real data's characteristics.

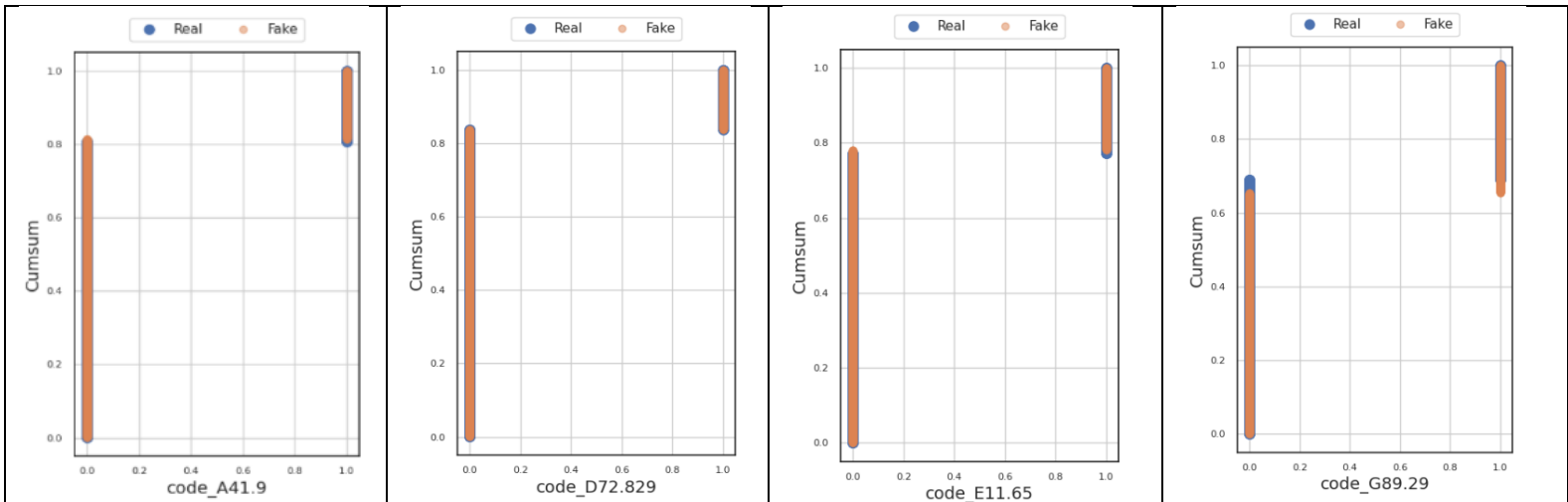
¹ Sepsis

² Elevated_WBC_count

³ T2DM_with_hyperglycemia

⁴ Chronic pain





Binary Gaussian Copula Synthesis

Figure 6: Comprehensive comparison between the distributions of real and fake data across feature set 1

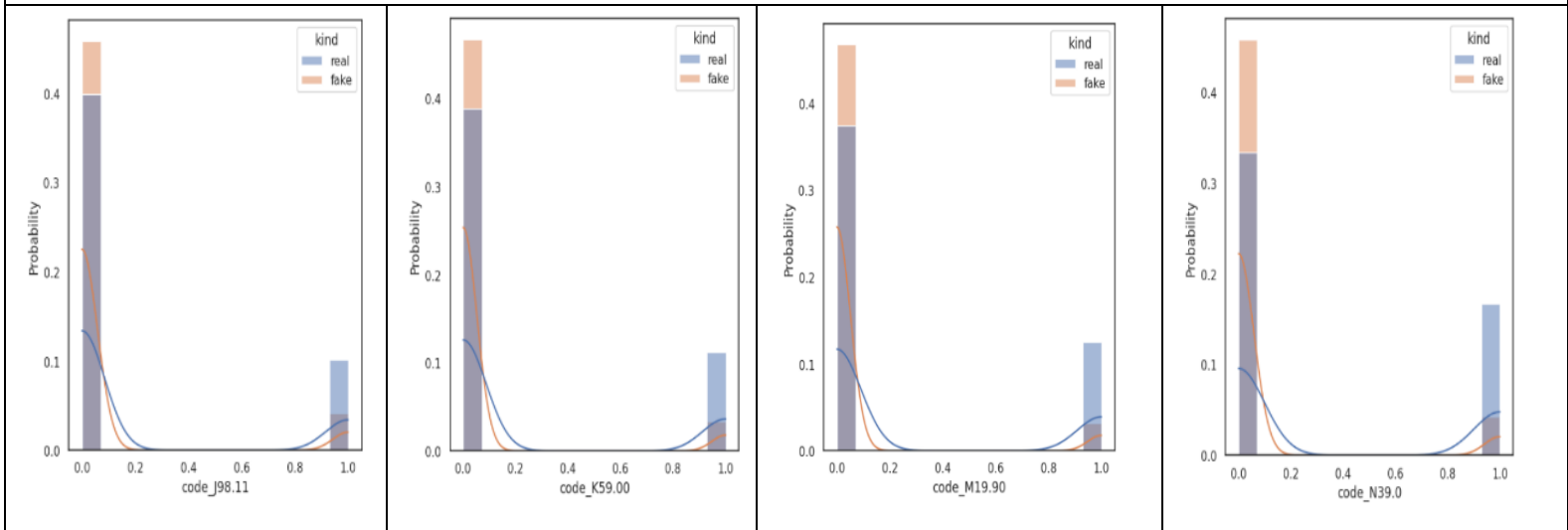
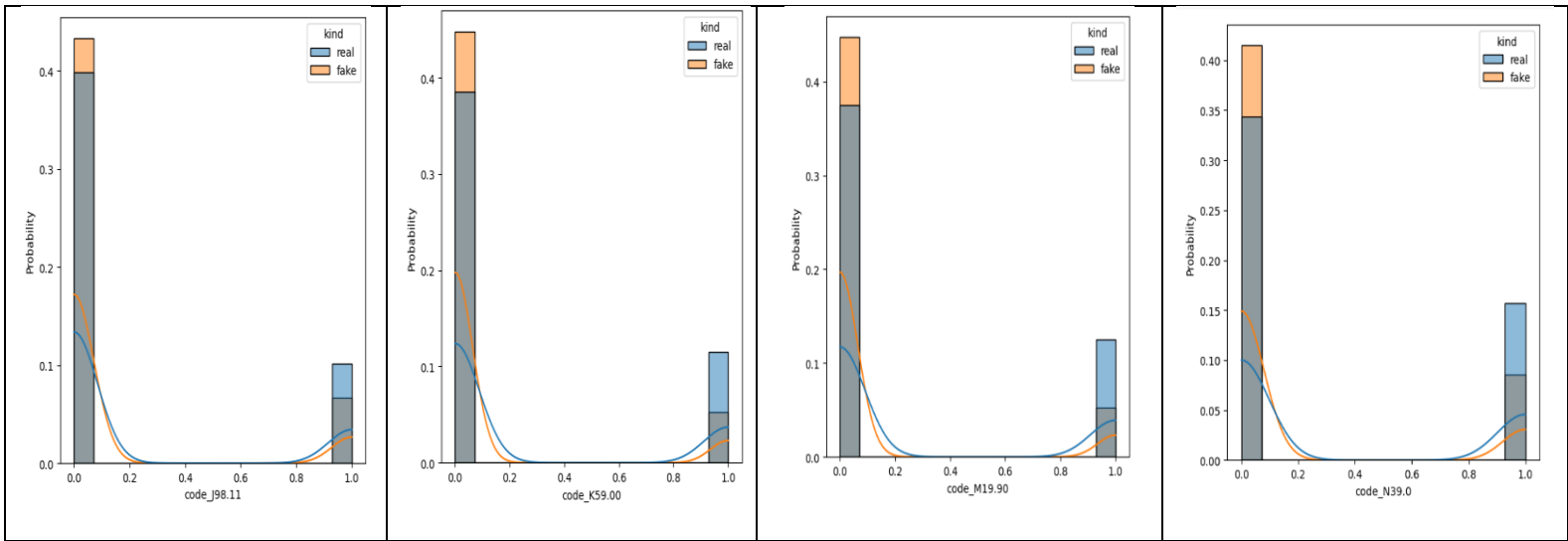
Figure 7 displays probability distribution plots for both real and synthetic data across feature set 2 including codes J98.11⁵, K59.00⁶, M19.90⁷, and N39.0⁸. The plot, using bars to represent the frequency of 0s and 1s, visualizes the distribution of binary variables that take values of either 0 or 1. The gray areas highlight the overlap between the real data (in blue) and the synthetic data (in orange), with lines representing the kernel density estimation (KDE). To validate an augmentation technique, it's crucial that the plot shows the synthetic data replicating the real data's distribution with minimal differences. Ideally, the probability distributions for both real and synthetic data should have a similar shape, meaning the bars (histograms) and KDE lines should closely align between the two datasets. As seen in this figure, the Gaussian Copula and BGCS methods seem to generate synthetic data that most closely mirrors the real data for the analyzed features, with BGCS showing a slightly superior performance. These methods are particularly effective in capturing the critical tails of distributions, which can represent rare but significant healthcare events. While CTGAN and SMOTE might be useful in other scenarios, they fall short of accurately reflecting the categorical distribution of the features as effectively as BGCS.

⁵ Vascular_dementia

⁶ Constipation_unspecified

⁷ Osteoarthritis_localized_involving_lower_leg

⁸ Other_disorders_urethra_UT



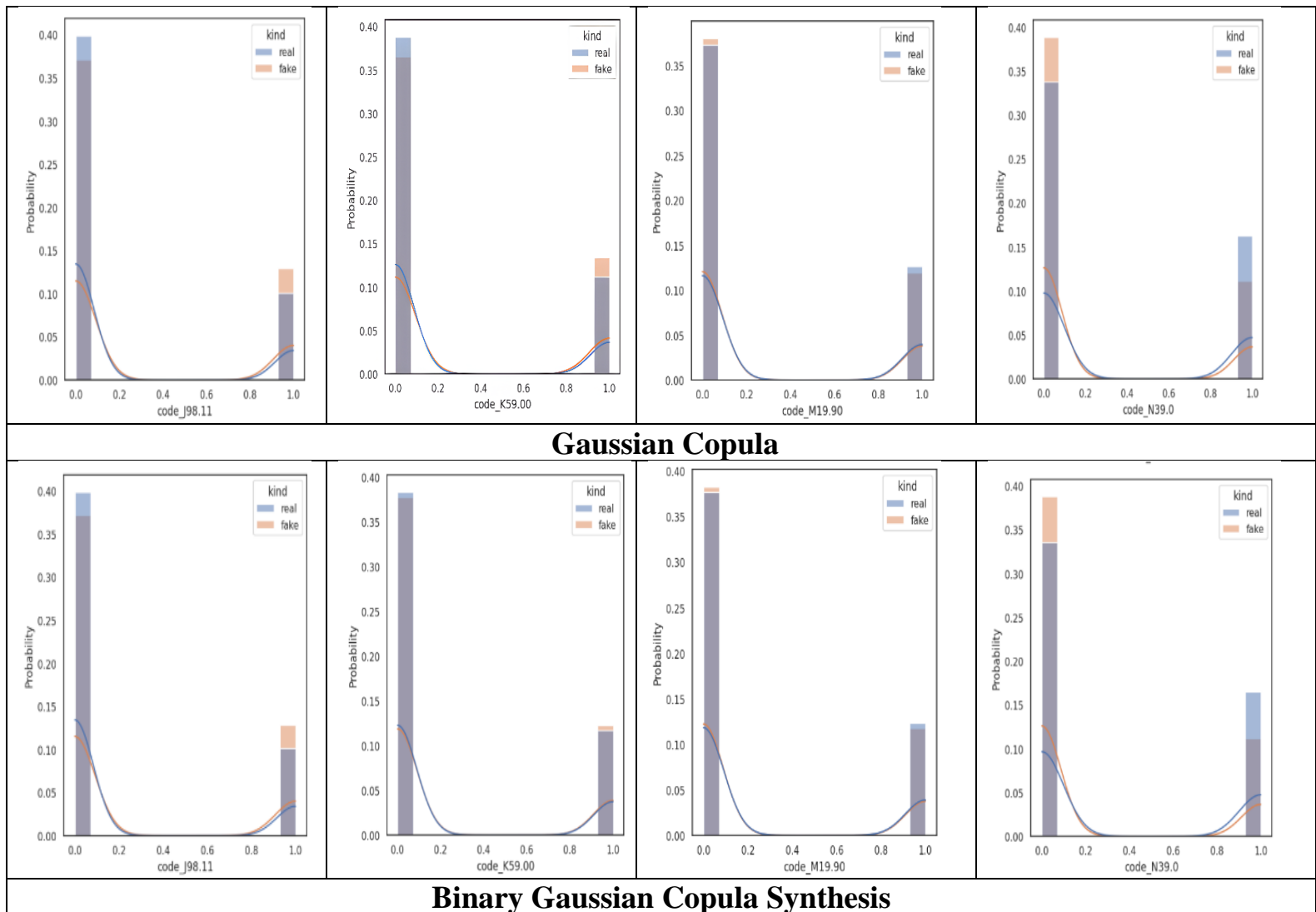


Figure 7: Comprehensive comparison between the distributions of real and fake data across feature set 2.

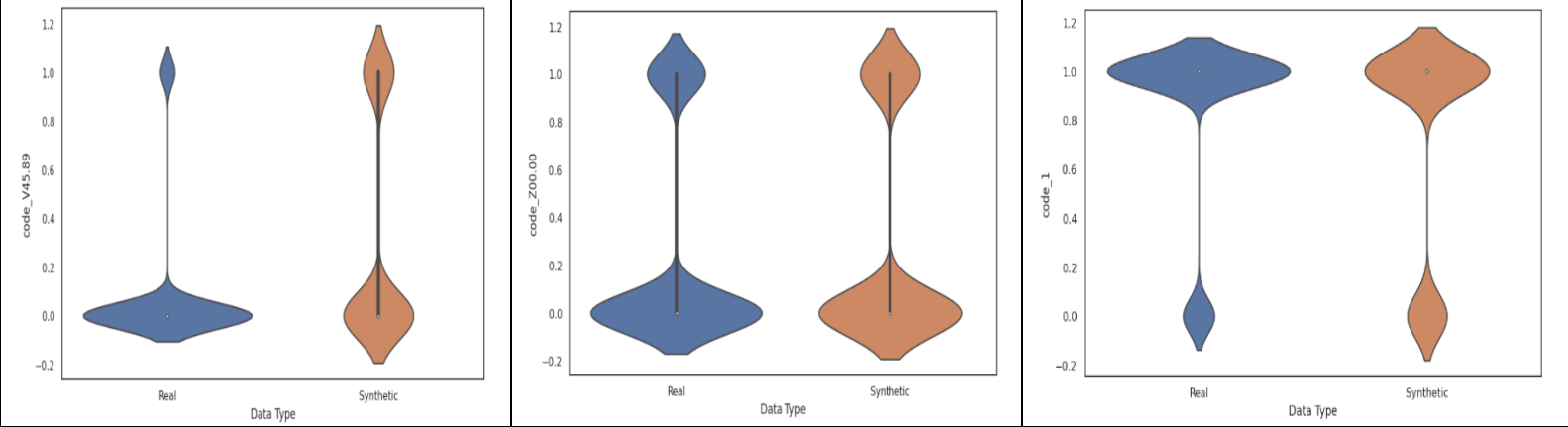
Figure 8 showcases a comparison of violin plots that illustrate the distributions of both real and synthetic data across the third feature set including codes V45.89⁹, Z00.00¹⁰, and 1¹¹. The similarity between the shapes of these violin plots is key to determining how well the synthetic data replicates the real data. For synthetic data to be considered effective, its corresponding violin plot should closely resemble the real data in terms of shape, width, and median. This resemblance indicates that the synthetic data accurately mirror the real data's distribution, density, and central tendency. From the analysis in this figure, the CTGAN technique shows a notable central tendency, but it may diverge from the median, leading to potential skewness in certain features like "V39.69." On the other hand, synthetic data generated by SMOTE tend to display less variance, as seen in "Z00.00," failing to capture the full spectrum of the actual data's diversity. In contrast, both Gaussian Copula and BGCS methods align more closely with the real data in terms of median and variance, offering a more accurate and comprehensive representation.

⁹ External_hearingaid

¹⁰ Routine_general_medical_examination

¹¹ Tablets

Gaussian Copula



Binary Gaussian Copula Synthesis

Figure 8: Comprehensive comparison between the distributions of real and fake data across feature set 3

Figure 8 showcases a comparison of violin plots that illustrate the distributions of both real and synthetic data. The similarity between the shapes of these violin plots is key to determining how well the synthetic data replicates the real data. For synthetic data to be considered effective, its corresponding violin plot should closely resemble the real data in terms of shape, width, and median. This resemblance indicates that the synthetic data accurately mirror the real data's distribution, density, and central tendency. From the analysis in this figure, the CTGAN technique shows a notable central tendency, but it may diverge from the median, leading to potential skewness in certain features like "V39.69." On the other hand, synthetic data generated by SMOTE tend to display less variance, as seen in "Z00.00," failing to capture the full spectrum of the actual data's diversity. In contrast, both Gaussian Copula and BGCS methods align more closely with the real data in terms of median and variance, offering a more accurate and comprehensive representation.

5.1.2. Statistical analysis

To enhance the univariate feature comparison made in the last sub-section, a binomial proportion test has been applied to both real and synthetic data. This test evaluates the ratio of values within the features, providing a more detailed assessment of how well the synthetic data replicates the real data's characteristics. To assess if the proportions in two datasets are equivalent, or if the difference between them is zero (given N_1 observations in X_1 and N_2 observations in X_2), the normal approximation test can be utilized. In this context, let p_1 and p_2 denote the percentages of 1's for the minor class in the real and synthetic data, respectively. The hypothesis test to determine if these two binomial proportions are equal can be structured as follows [95]:

$$\begin{aligned}
 H_0: & \quad p_1 = p_2 \\
 H_1: & \quad p_1 \neq p_2 \\
 \text{Test Statistic:} & \quad Z = \frac{\hat{p}_1 - \hat{p}_2}{\sqrt{\hat{p}(1-\hat{p})(1/n_1 + 1/n_2)}}
 \end{aligned} \tag{21}$$

where \hat{p} stands for the ratio of 1's for the combined real and synthetic data and is calculated by

the equation (22):

$$\hat{p} = \frac{n_1\hat{p}_1+n_2\hat{p}_2}{n_1+n_2} = \frac{X_1+X_2}{n_1+n_2} \quad (22)$$

In this test, the significance level is α and critical region is shown as:

$$\begin{aligned} Z &> \Phi^{-1}(1 - \alpha/2) \\ Z &< \Phi^{-1}(\alpha/2) \end{aligned} \quad (23)$$

If the calculated Z-statistic value falls within the critical region, then the null hypothesis (H_0) is rejected, indicating a significant difference between the proportions in the real and synthetic data. For a data augmentation method to be considered effective, the null hypothesis should not be rejected, suggesting that the synthetic data mirrors the ratio of the real data. Table 5 offers a comprehensive comparison of the methods by summarizing the test results across all features, using six different significance levels (**Please refer to Appendix B for an in-depth comparison**).

Table 5: Comprehensive comparison of methods across all features at six significance levels: Summary of Binomial proportion test results

	SMOTE	CTGAN	Gaussian Copula	BGCS
Z-Statistic Range	(2.40, 13.47)	(-9.21,6.80)	(-2.88, 0.98)	(-1.40, 1.31)
Z-Statistic Mean	6.29	-0.99	-0.39	-0.26
Z-Statistic Std	1.82	4.30	0.71	0.46
P-Value Range	(2.33E-41, 1.62E-02)	3.33E-20, 9.96E-01	3.85E-3, 0.99	0.15, 0.99
P-value Mean	2.23E-04	8.01E-02	0.57	0.67
P-value Std	1.59E-03	1.88E-01	0.26	0.19
Number of Dissimilar Instances	953	773	97	37
Number of Similar Instances	7	187	863	923

Table 5 provides a comprehensive statistical analysis, comparing four data augmentation techniques across 960 different scenarios, derived from 160 features at six varying significance levels (alphas). This analysis reveals notable differences among the methods. SMOTE shows a broad range of Z-statistics (from 2.402316 to 13.470381), indicating significant variability, whereas BGCS exhibits a narrower range (from -1.407019 to 1.316828), suggesting more consistent replication of the real data's proportions. BGCS has emerged as the superior method with the highest average p-value (0.675505), indicating a closer alignment between the synthetic and real data's proportions, as lower statistical significance suggests a better match. This is further supported by the number of instances deemed to have similar proportions, with BGCS correctly identifying 923 similar instances (96%). In comparison, CTGAN, SMOTE, and Gaussian Copula identify significantly fewer similar instances, with counts of 187, 7, and 863, respectively. These findings highlight BGCS as the most effective method in mirroring the feature distributions of real data without significant statistical discrepancies. To provide a more thorough assessment of the methods' effectiveness, a full feature space analysis is conducted in the subsequent section.

5.1.3. Full space feature analysis

This subsection presents a comprehensive comparison of data augmentation methods using t-SNE and PCA, encompassing the full spectrum of features in the dataset. The effectiveness of each method is assessed by comparing the structural integrity of the synthetic data against the original dataset. This comparative analysis is crucial for understanding how well these techniques preserve the complex relationships and inherent patterns found in the real data. Figure 9 displays these comparisons using t-SNE with a perplexity value of 30, balancing the attention between local and global aspects of the data to influence how the data points group together in the visualization. The choice of perplexity levels allows for a nuanced view of how each augmentation method performs in maintaining the data's multidimensional structure (**Please refer to Appendix C for other values of perplexity values**).

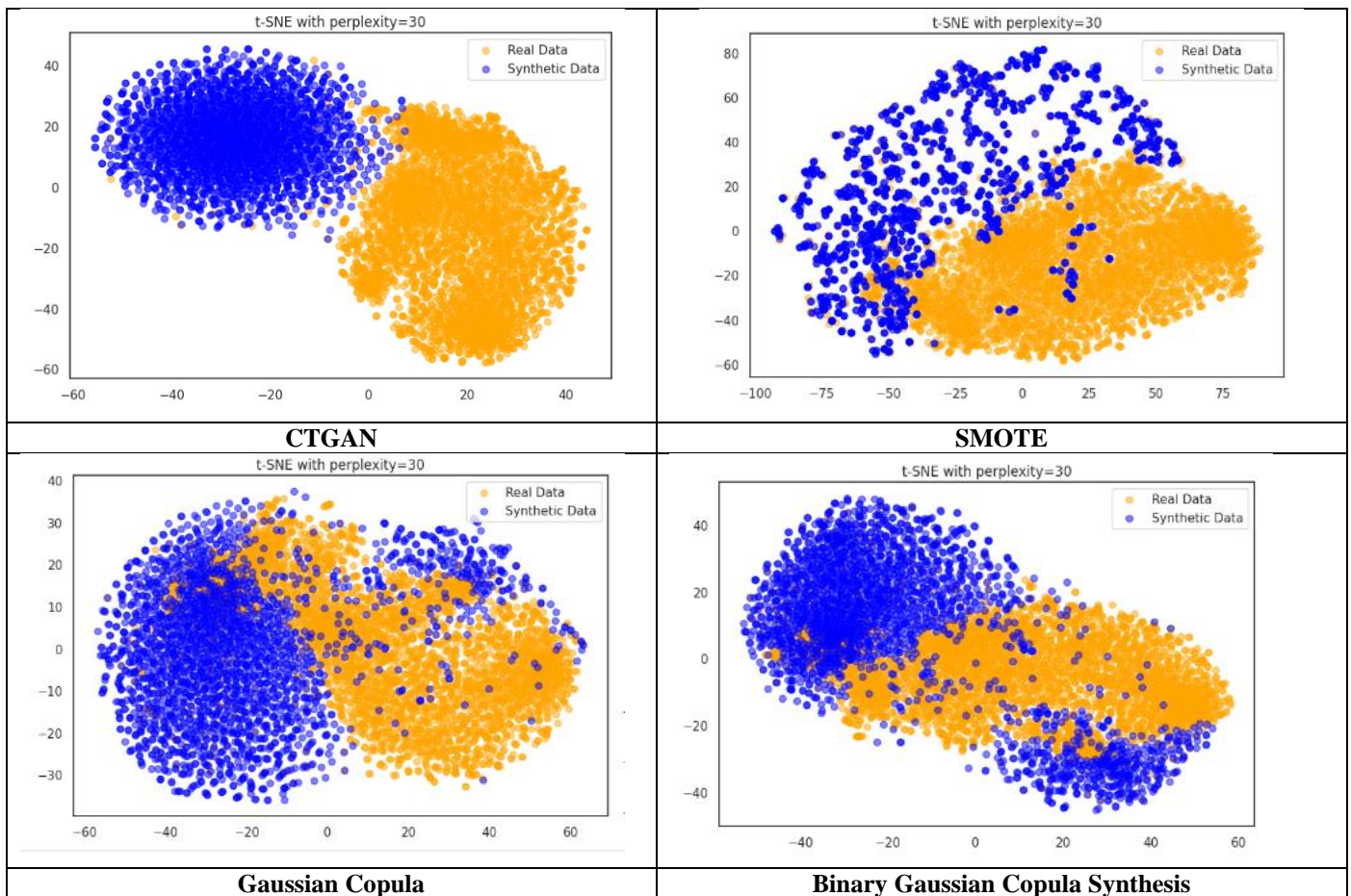


Figure 9: Comprehensive comparison between the real and fake data considering t-sne (medium perplexity)

By projecting high-dimensional data into a two-dimensional space, t-SNE enables an intuitive comparison of the distributional characteristics between original and augmented data sets. Real data points are displayed in blue and augmented, and synthetic data points are displayed in orange on the plots generated. An effective data augmentation method should show substantial overlap between the two sets of points, indicating that the synthetic data provides the same complex

structure as the original data. In Figure 9, which balances local and global structures, the CTGAN plot begins to integrate real and synthetic data better, although it is still visible that clear clusters of separation exist. There is a widespread diffusion of synthetic points throughout SMOTE's representation, implying a lack of distinct data groupings. As indicated by the Gaussian Copula visualization, data overlap has improved moderately, with synthetic data starting to closely resemble real data's global structure. The BGCS maintains a high level of integration, demonstrating its ability to retain the overall structure of the data. BGCS demonstrates consistently superior performance in replicating complex data structures in t-SNE analysis. In contrast, other methods like CTGAN and SMOTE struggle with accurately representing local data structures, while the Copula method shows improvement as the complexity increases. Following this, Figure 10 provides a visual comparison of real and synthetic data through PCA, focusing on the first two principal components, and offering further insights into the effectiveness of these data augmentation methods.

Figure 10 illustrates the extent to which each data augmentation technique captures the variance and structure of the real data. An analysis of the PCA plot for real data reveals a broad and somewhat heart-shaped distribution of features in the transformed feature space. The data ranges on the x-axis from about -4 to 6 and on the y-axis from approximately -3 to 3. Accordingly, CTGAN generates synthetic data clouds that are significantly denser and more centralized, with the majority of data points falling within the -2 to 2 range on both axes suggesting that CTGAN is somewhat conservative in capturing the full range of variance. SMOTE's synthetic data, on the other hand, exhibit a wider distribution than the real data spanning from -2 to 6 on the x-axis and -3 to 4 on the y-axis. The dispersion indicates that SMOTE may overestimate the variability within the data, potentially resulting in synthetic datasets that are too dispersed. It appears that Copula-generated data is well matched to the real data's distribution on the y-axis, ranging from -3 to 3, but there is a slight contraction on the x-axis, ranging from about -4 to 4. Through the Gaussian Copula method, synthetic data can be generated with distribution patterns that are very similar to those of real data, matching both the density and orientation of the clusters. Consequently, the Gaussian Copula method is effectively used to model the primary axes of variation in the dataset. Lastly, BGCS-augmented data is closely aligned with the real data, providing high fidelity in the representation of the shape and orientation of the data cloud, extending from -4 to 6 on the x-axis and -3 to 3. Therefore, BGCS provides a balanced representation of variance and structure in order to capture the complex relationships between features.

5.1.4. Performance analysis

Using ML models trained on datasets augmented with synthetic data, the efficacy of data augmentation techniques is further evaluated in this section. In Figure 11, we examine the class balance before and after data augmentation, specifically by creating synthetic instances for the dialysis class which has been underrepresented. During this process, the dataset is meaningfully enhanced to ensure a more equitable distribution of classes, thereby improving its suitability for ML models.

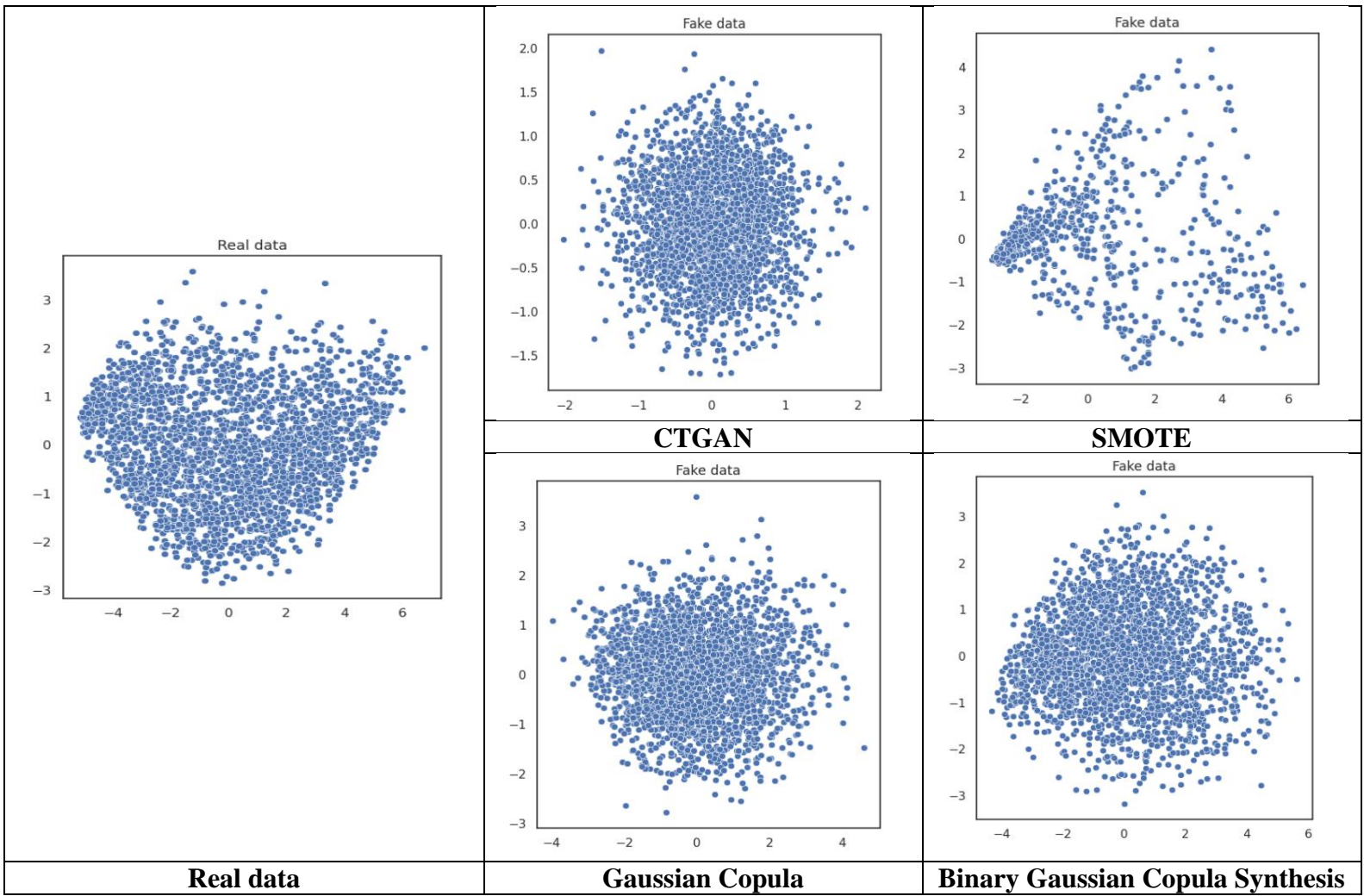


Figure 10: Comparison between the real and fake data considering the first two components of PCA



Figure 11: Comparison between the ratio of the classes before and after data generation

To emphasize the significance of data augmentation when addressing class imbalance, particularly for minority class, Figure 12 shows the recall scores for the dialysis class based on different ML models, with evaluations conducted over a period of 25 runs.

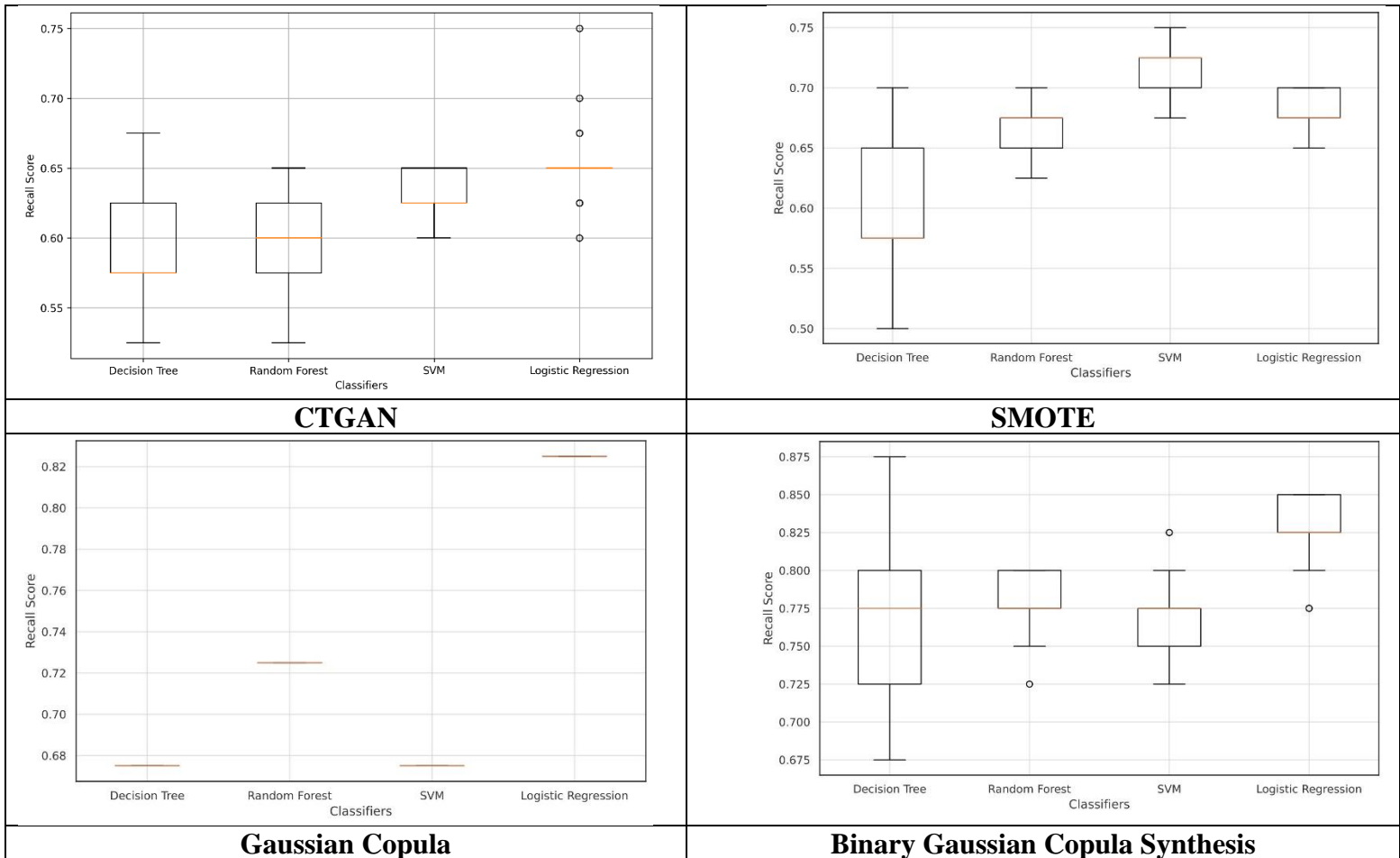


Figure 12: Comparison between different models considering different data augmentation techniques.

According to Figure 12, the performance of classifiers on CTGAN-augmented data ranges from approximately 0.58 to 0.62, with Decision Trees showing the greatest interquartile range (IQR), indicating that the model exhibits variability in performance. The Logistic Regression indicates a tighter IQR, which indicates a more consistent recall score. A slight difference in median recall between the classifiers is observed with SMOTE-augmented data, ranging from 0.63 to 0.67. The expanded IQRs of the decision tree suggest variability in recall scores, suggesting that the model performance can be unstable across different runs based on the expanded IQRs. Utilizing Gaussian Copula to generate data, there is an improvement in recall with a median score hovering around 68 to 0.82 for the classifiers. The median recall scores for BGCS-augmented datasets are approximately 0.78 to 0.82 across all classifiers. In particular, the compact IQRs observed with the Random Forest and Logistic Regression models indicate a high degree of precision and reliability in detecting the minority class. As a result, it is clear that for the minority group, BGCS outperforms other methods in terms of recall, suggesting that it is effective at creating synthetic data that can be used to develop more sensitive and reliable prediction models. To illustrate the

improvement achieved by the data augmentation techniques, Figure 13 shows the comparison of all ML models trained on augmented datasets and real data.

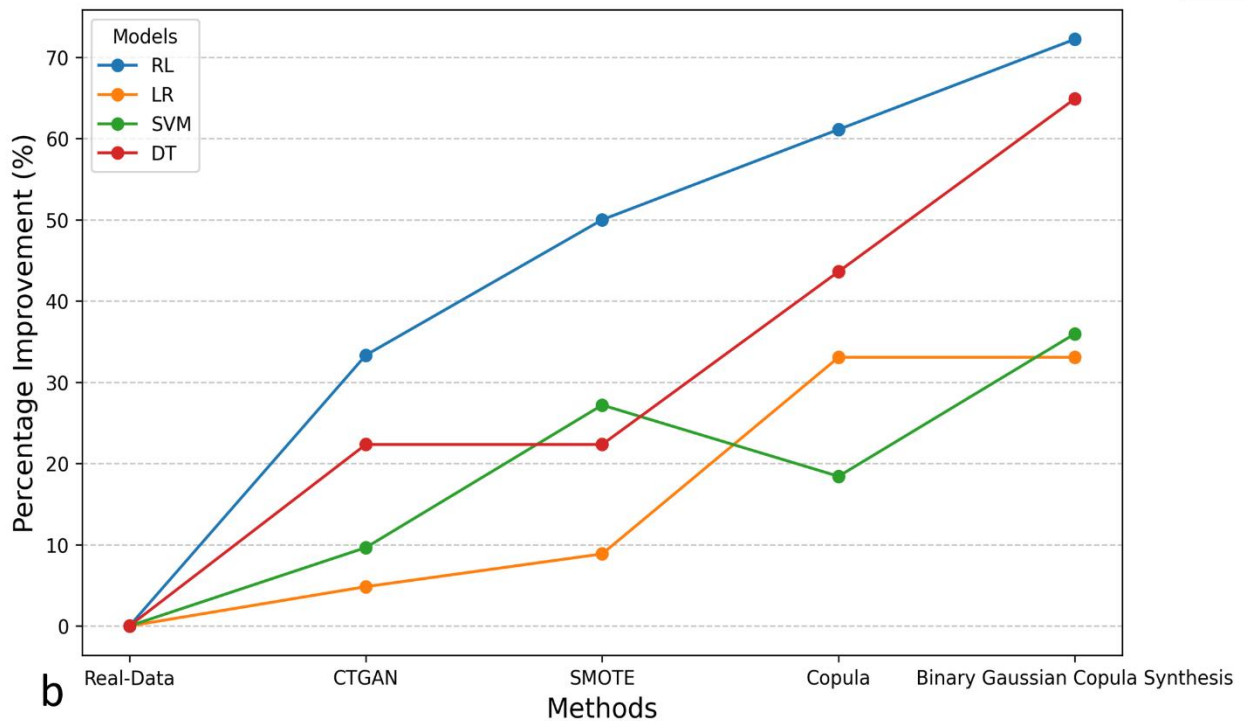
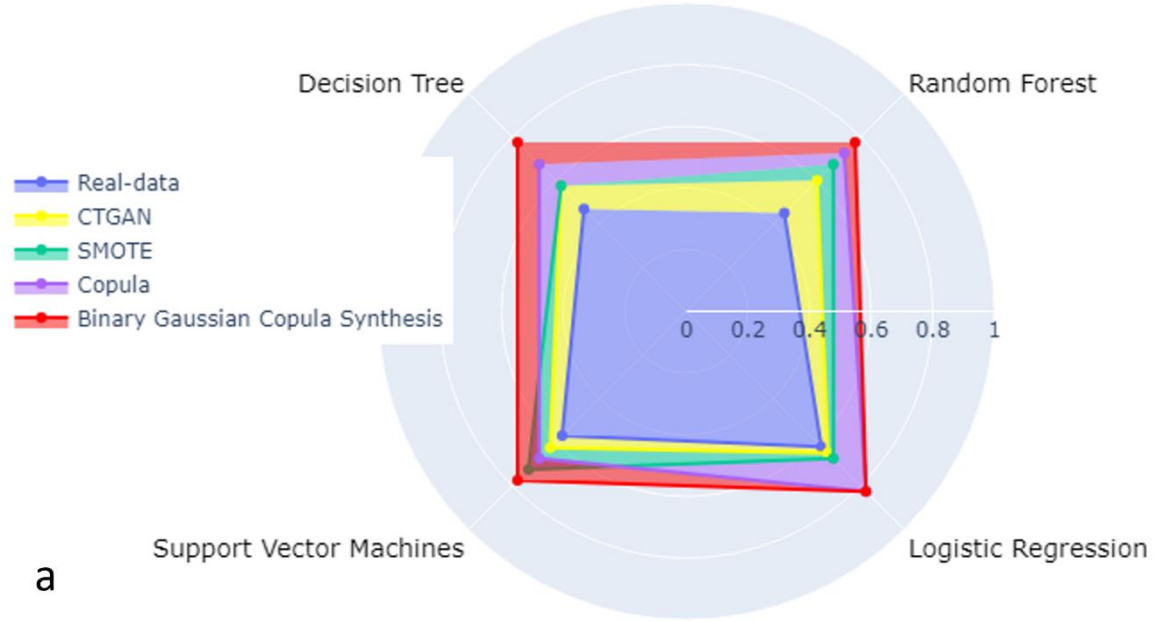


Figure 13: Comparison of models' recall using different data augmentation techniques and real data. (a) Radar chart illustrating the recall of the ML models on real and augmented datasets (b) Line graph showing the recall improvement trends for each model trained on real data and augmented data

In the radar chart (a), the recall spread for each classifier is shown, with each axis representing a different model. The closer the lines are to the chart's outer perimeter, the higher the recall value. In comparison to other techniques, BGCS augmented models have lines that are closer to the edges, which indicates higher recall values, whereas lines that are closer to the edges indicate lower recall values. Line graph (b) depicts how recall has improved for each ML model when being trained on datasets supplemented with different data generation techniques compared to the baseline recall achieved using real data. Across all models, the BGCS method consistently leads to a greater recall, which indicates a significant improvement over the real data analyzed, ranging from 32% to 72% improvement. In addition to BGCS, other augmentation techniques such as CTGAN, SMOTE, and Copula have also improved recall, but at a lower level. These methods have relatively flat lines, suggesting that even though they contribute to an improved recall, the extent of this improvement does not vary significantly between models. In contrast, the BGCS line exhibits a higher recall value at each model point, demonstrating its effectiveness across a range of ML models.

5.2. CDSS development

The BGCS method of data augmentation stands out for significantly enhancing the performance of ML models compared to other techniques. As a result, datasets augmented with BGCS are chosen for further analysis in the development of the CDSS. Given the vital need for interpretability in clinical settings, the Decision Tree algorithm is selected as the foundation for the CDSS. This choice is driven by its ability to foster user trust and provide actionable insights, both of which are crucial in clinical applications.

Figure 14, using the recall metric, demonstrates the impact of BGCS-augmented data on the performance of a decision tree model. The figure features a red line representing the recall achieved with real data (0.47), contrasted by a green line (black boxplot) showing the significantly improved recall with augmented data (mean=0.76, median=0.78). This indicates that the BGCS method effectively combats the issue of class imbalance, resulting in a more robust and accurate decision tree model, particularly for the minority class. Notably, the model with a median recall of 0.78 (orange line) was chosen as the foundation for the development of the CDSS) aimed at early dialysis prediction.

Figure 15 depicts a truncated decision tree, emphasizing the hierarchical positioning of features in the model rather than their ultimate decisiveness in class prediction. The figure highlights "code_G0480" at the root node with a Gini threshold of 0.494, indicating its prominence in initial data separation rather than its overall importance in class determination. "Code_G0480," representing drug identification methods for individual drugs and structural isomers, primarily influences the model's preliminary branching. At the second level, "code_Z09" (indicative of follow-up examinations for conditions other than malignant neoplasm) and "code_85025" (complete blood count), appear with Gini thresholds of 0.321 and 0.478, respectively. This reflects their role in further data segmentation within the model, rather than reflecting their significance in the dialysis prediction. To enhance the interpretability and efficiency of the model, it's crucial to comprehend these factors that significantly impact the model's predictions. However, it is important to note that while the top few variables ("code_G0480", "code_Z09", "code_85025") in a decision tree are instrumental in understanding the overall branching process, they may not always be the most critical for class prediction. The variables that effectively distinguish between classes, such as dialysis and non-dialysis in our case, are of greater importance for accurate class separation. These essential variables, which play a pivotal role in differentiating between classes,

are discussed in detail on the following page. An illustration of the comprehensive framework of the proposed CDSS is provided in Figure 16, which illustrates how ML techniques can be integrated to assist medical professionals in the early prediction process.

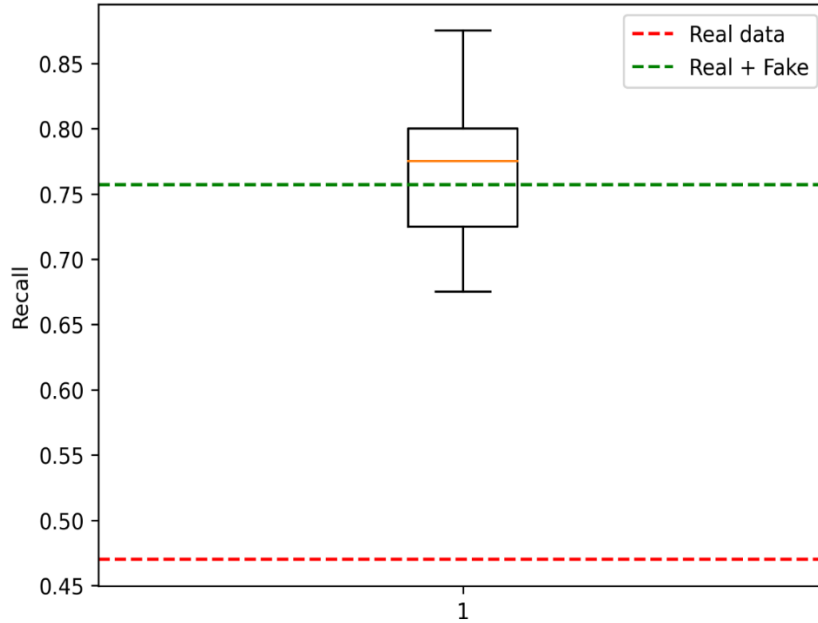


Figure 14: Improvement using BGCS-augmented data trained on decision tree model

In developing the CDSS for our case, early prediction of dialysis need is prioritized, and a series of rigorous steps is implemented to ensure the robustness and clinical relevance of the system.

- **Data Preparation:** After handling the missing values, we carefully select features to maximize predictive power while emphasizing clinical relevance. To enable early prediction, data from the most recent 90 days is excluded to focus on leading indicators.
- **Class imbalance assessment and mitigation:** To ensure sufficient representation of dialysis class for model training, data augmentation techniques are utilized.
- **Augmentation validity confirmation:** Univariate and full feature space analysis rigorously ensure the statistical validity of the augmented data compared to the real data.
- **Models Evaluation:** Evaluation of models' performance is conducted by training the model on the augmented data, which results in significant improvements in minority class recall, the key performance indicator for our analysis.
- **Interpretable AI:** We select the decision tree based on its interpretability, which allows clinicians to understand the overall branching and reasoning behind each prediction. By using binary decisions based on medical codes, the decision tree model identifies patients who are more likely to require dialysis. Using a mathematical model, the prediction capability of the decision tree can be abstracted into a binary target variable, D representing dialysis, and binary input variables, X_1, X_2, \dots, X_n (n =number of features) representing medical codes. The decision process follows a function f :

$$f(X_1, X_2, \dots, X_n) = P(D = 1) = \begin{cases} p_1 & \text{if } X_1 \leq 0.50 \wedge \dots \wedge X_j \leq 0.50 \\ p_2 & \text{if } X_1 > 0.50 \wedge \dots \wedge X_j \leq 0.50 \wedge \dots \wedge X_k > 0.50 \\ \vdots & \\ p_m & \text{if } X_1 > 0.50 \wedge \dots \wedge X_k > 0.50 \end{cases} \quad (24)$$

Here, p_i corresponds to the probability of the patient requiring dialysis under each specific combination of medical code states.

- Decision-making:** To aid clinicians in making informed decisions, using equation 24, we have identified the most decisive features, offering them timely, data-driven insights. The model prioritizes medical codes hierarchically, underscoring their importance in predicting the onset of dialysis in the near future. Table 6 lists the top 10 crucial features, along with their interpretations, as determined by the decision tree model. These codes are essential for identifying and assessing dialysis outcomes, as they are likely linked to particular clinical interventions or complications. This approach streamlines the decision-making process by highlighting the key factors that influence dialysis requirements.

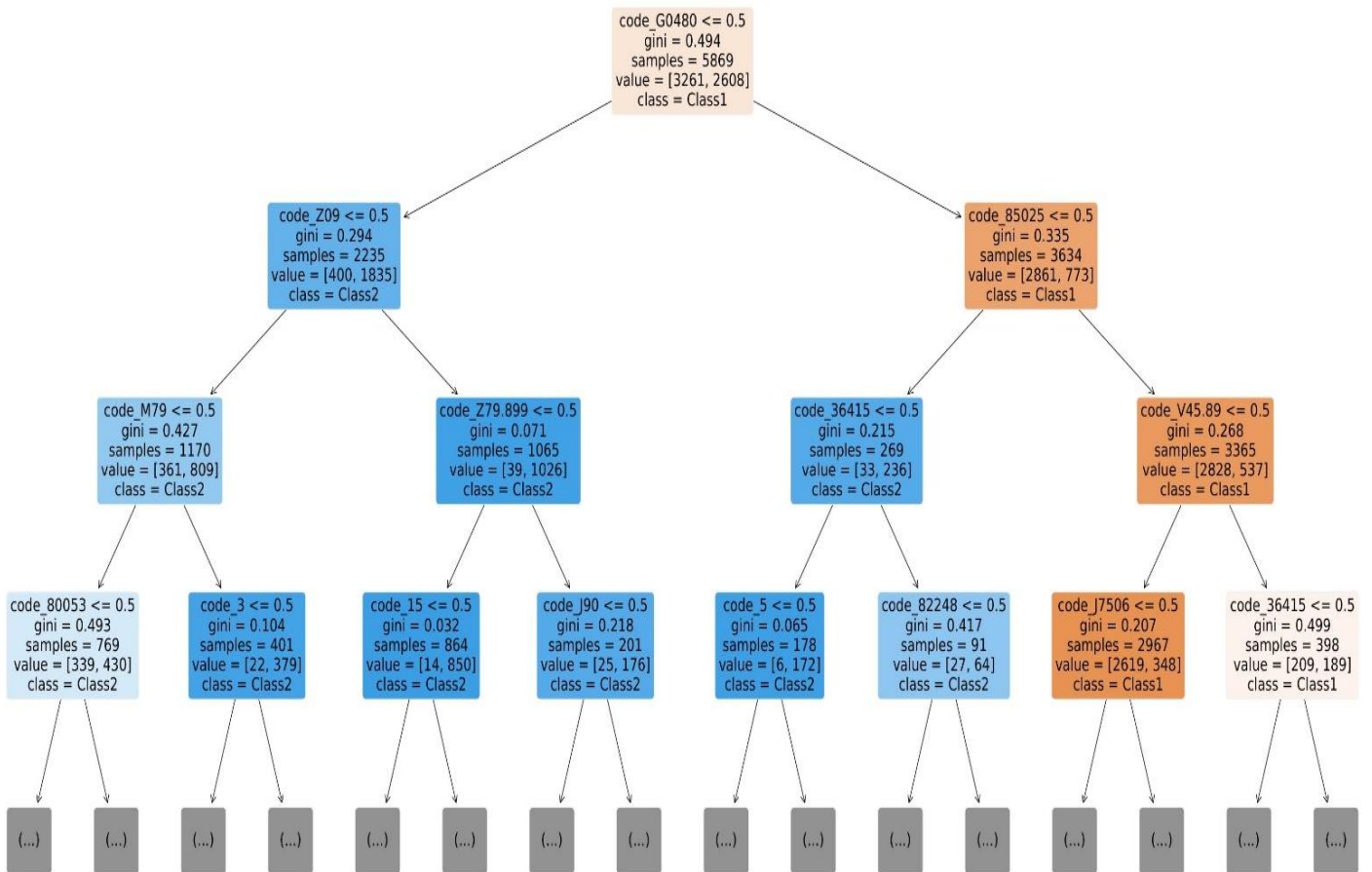


Figure 15: The tree structure of the model applied on BGCS-augmented data used in the CDSS

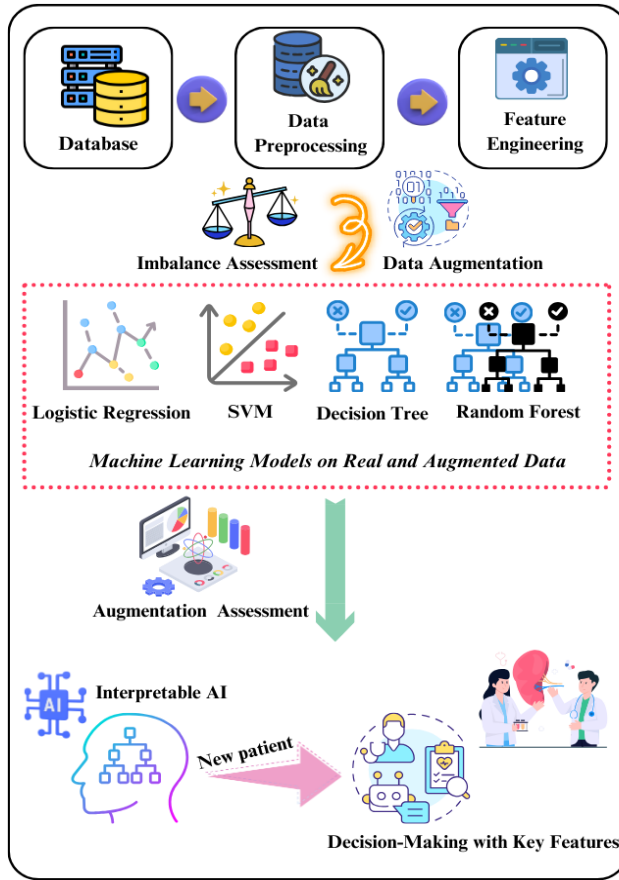


Figure 16: Overall framework of the proposed CDSS

Table 6: Top 10 key features extracted from the decision tree model for dialysis prediction

Code	Representation
E87.5	Hyperkalaemia
E87.6	Hypokalaemia
I25.2	Myocardial infarction
I10	Hypertension
81001	Urinalysis, by dip stick or tablet reagent for bilirubin, glucose, haemoglobin, ketones, leukocytes, nitrite, pH, protein, specific gravity, urobilinogen, any number of these constituents.
84100	Level of phosphate in a patient specimen such as serum
I11.0	Hypertensive_heartdisease_with_HF
84295	Sodium concentration
I51.7	Cardiomegaly
R94.31	Nonspecific_abnormal_ECG_EKG_

In the context of CKD, the CDSS is particularly important in improving the decision-making process, as early and accurate prediction of dialysis can result in substantial patient benefits. By

integrating BGCS-augmented datasets, the system effectively addresses the class imbalance problem inherent in CKD data, primarily where dialysis instances are relatively rare compared to the overall patient population. Using this balanced data representation, the proposed CDSS can identify potential dialysis cases before they become critical, enabling timely and preventative measures to be taken. Furthermore, the system's ability to identify early indicators of CKD progression is further enhanced by the use of advanced data preparation techniques and feature engineering. This proactive approach to disease management not only provides clinicians with foresight but also allows them to strategize treatment plans more effectively, thus potentially preventing the onset of severe stages of CKD. However, it is important to note that the CDSS, enriched by datasets augmented with BGCS techniques, is designed as an auxiliary tool, not to replace clinical judgment. Recommendations, especially regarding dialysis, should be considered alongside medical expertise. It is crucial to conduct an in-depth case-by-case analysis that incorporates clinician judgment, as well as CDSS insights, to optimize patient care.

6. Conclusions and Future Work

This study represents a significant leap forward in managing CKD by developing a ML-based CDSS for the 90-days early prediction of dialysis. A key innovation of this research is the introduction of the novel Binary Gaussian Copula Synthesis (BGCS) method, effectively tackling the issue of class imbalance in CKD datasets. The BGCS method not only preserves the structural integrity and statistical distribution of the original data but also enriches it by adding realistic and representative instances of the minority class. This enhancement is particularly crucial for early dialysis prediction, where our findings show a marked improvement in model recall, especially for this critical minority class.

When compared to traditional data augmentation techniques like CTGAN, SMOTE, and Gaussian Copula, BGCS stands out for its superior performance across various ML models, achieving a median recall range of 0.78 to 0.82. This method has proven to be the most effective for data augmentation, significantly enhancing the performance of models like Random Forest and Decision Tree (improvements of 72% and 65%, respectively) when trained on BGCS-augmented datasets versus real data. The consistently high recall values underscore BGCS's effectiveness in boosting model sensitivity towards the minority class. The integration of BGCS-augmented datasets into the proposed CDSS is a strategic move to address the imbalance in CKD data, enabling early detection of potential dialysis cases. Thus, BGCS not only bolsters the performance of predictive models but also significantly enhances the practicality of our CDSS in clinical environments. Equipped with BGCS, the CDSS serves as a valuable addition to the clinician's expertise, marking a pivotal advancement in personalized patient care for CKD. It offers actionable insights through the identification of important variables that are crucial for early intervention in dialysis cases.

Looking ahead, the application of the CDSS and BGCS in broader healthcare datasets opens avenues for future research, particularly in clinical validation. This will solidify their role as essential tools in predictive healthcare analytics. Further refinement of distributional comparisons between real and synthetic datasets could be achieved by incorporating kernel-based distance measures such as those described in the literature [96,97]. Additionally, exploring hybrid data augmentation methods, such as combining VAE with Copulas and GANs with Copulas, holds

promise for further enhancing the quality and clinical applicability of synthetic data across diverse medical scenarios.

Acknowledgments

We would like to express our profound appreciation to the Department of Industrial & Management Systems Engineering (IMSE), WVU for their consistent and invaluable support during this research project.

Fundings

This work was supported by the WVU Benjamin M. Statler College of Engineering and Mineral Resources.

References

- [1] W. Lee and K. Seo, "Downsampling for Binary Classification with a Highly Imbalanced Dataset Using Active Learning," *Big Data Research*, vol. 28, p. 100314, May 2022, doi: <https://doi.org/10.1016/j.bdr.2022.100314>.
- [2] T. M. Alam *et al.*, "An Efficient Deep Learning-Based Skin Cancer Classifier for an Imbalanced Dataset," *Diagnostics*, vol. 12, no. 9, p. 2115, Sep. 2022, doi: <https://doi.org/10.3390/diagnostics12092115>.
- [3] D. S. Rajput *et al.*, "Providing diagnosis on diabetes using cloud computing environment to the people living in rural areas of India," *Journal of Ambient Intelligence and Humanized Computing*, vol. 13, Apr. 2021, doi: <https://doi.org/10.1007/s12652-021-03154-4>.
- [4] L. Gao, L. Zhang, C. Liu, and S. Wu, "Handling imbalanced medical image data: A deep-learning-based one-class classification approach," *Artificial Intelligence in Medicine*, vol. 108, p. 101935, Aug. 2020, doi: <https://doi.org/10.1016/j.artmed.2020.101935>.
- [5] M. Galar, A. Fernandez, E. Barrenechea, H. Bustince, and F. Herrera, "A Review on Ensembles for the Class Imbalance Problem: Bagging-, Boosting-, and Hybrid-Based Approaches," *IEEE Transactions on Systems, Man, and Cybernetics, Part C (Applications and Reviews)*, vol. 42, no. 4, pp. 463–484, Jul. 2012, doi: <https://doi.org/10.1109/tsmcc.2011.2161285>.
- [6] A. Islam, S. B. Belhaouari, A. U. Rehman, and H. Bensmail, "KNNOR: An oversampling technique for imbalanced datasets," *Applied Soft Computing*, vol. 115, p. 108288, Jan. 2022, doi: <https://doi.org/10.1016/j.asoc.2021.108288>.
- [7] JapkowiczNathalie and StephenShaju, "The class imbalance problem: A systematic study," *Intelligent Data Analysis*, vol. 6, no. 5, Oct. 2002, doi: <https://doi.org/10.5555/1293951.1293954>.
- [8] G. Vandewiele *et al.*, "Overly optimistic prediction results on imbalanced data: a case study of flaws and benefits when applying over-sampling," *Artificial Intelligence in Medicine*, vol. 111, p. 101987, Jan. 2021, doi: <https://doi.org/10.1016/j.artmed.2020.101987>.
- [9] W. Lee and K. Seo, "Early failure detection of paper manufacturing machinery using nearest neighbor-based feature extraction," *Engineering Reports*, vol. 3, no. 2, Sep. 2020, doi: <https://doi.org/10.1002/eng2.12291>.
- [10] S. Liu, Y. Wang, J. Zhang, C. Chen, and Y. Xiang, "Addressing the class imbalance problem in Twitter spam detection using ensemble learning," *Computers & Security*, vol. 69, pp. 35–49, Aug. 2017, doi: <https://doi.org/10.1016/j.cose.2016.12.004>.
- [11] S. Dhankhad, E. Mohammed, and B. Far, "Supervised ML Algorithms for Credit Card Fraudulent Transaction Detection: A Comparative Study," *IEEE Xplore*, Jul. 01, 2018. <https://ieeexplore.ieee.org/abstract/document/8424696>
- [12] L. J. Mena and J. A. Gonzalez, "ML for Imbalanced Datasets: Application in Medical Diagnostic," *Conference: Proceedings of the Nineteenth International Florida Artificial Intelligence Research Society Conference*, pp. 574–579, Jan. 2006.
- [13] V. Kumar *et al.*, "Addressing Binary Classification over Class Imbalanced Clinical Datasets Using Computationally Intelligent Techniques," *Healthcare*, vol. 10, no. 7, p. 1293, Jul. 2022, doi: <https://doi.org/10.3390/healthcare10071293>.
- [14] M. Saarela, O.-P. Ryynänen, and S. Äyrämö, "Predicting hospital associated disability from imbalanced data using supervised learning," *Artificial Intelligence in Medicine*, vol. 95, pp. 88–95, Apr. 2019, doi: <https://doi.org/10.1016/j.artmed.2018.09.004>.
- [15] M. Khushi *et al.*, "A Comparative Performance Analysis of Data Resampling Methods on Imbalance Medical

- Data,” *IEEE Access*, vol. 9, pp. 109960–109975, 2021, doi: <https://doi.org/10.1109/access.2021.3102399>.
- [16] Ayodeji Olalekan Salau, Elisha Didam Markus, Tsehay Admassu Assegie, Crescent Onyebuchi Omeje, and Joy Nnenna Eneh, “Influence of Class Imbalance and Resampling on Classification Accuracy of Chronic Kidney Disease Detection,” *Mathematical modelling of engineering problems*, vol. 10, no. 1, pp. 48–54, Feb. 2023, doi: <https://doi.org/10.18280/mmep.100106>.
- [17] N. Norori, Q. Hu, F. M. Aellen, F. D. Faraci, and A. Tzovara, “Addressing bias in big data and AI for health care: A call for open science,” *Patterns*, vol. 2, no. 10, p. 100347, Oct. 2021, doi: <https://doi.org/10.1016/j.patter.2021.100347>.
- [18] J. Yang, A. A. S. Soltan, D. W. Eyre, and D. A. Clifton, “Algorithmic fairness and bias mitigation for clinical ML with deep reinforcement learning,” *Nature Machine Intelligence*, vol. 5, no. 8, pp. 884–894, Aug. 2023, doi: <https://doi.org/10.1038/s42256-023-00697-3>.
- [19] H. Salehinejad, S. Valaee, T. Dowdell, E. Colak, and J. Barfett, “Generalization of Deep Neural Networks for Chest Pathology Classification in X-Rays Using Generative Adversarial Networks,” *IEEE Xplore*, Apr. 01, 2018. <https://ieeexplore.ieee.org/abstract/document/8461430> (accessed Feb. 21, 2022).
- [20] Centers for Disease Control and Prevention, “Chronic Kidney Disease Basics,” *Centers for Disease Control and Prevention*, Feb. 28, 2022. <https://www.cdc.gov/kidneydisease/basics.html>
- [21] C. P. Kovesdy, “Epidemiology of Chronic Kidney disease: an Update 2022,” *Kidney International Supplements*, vol. 12, no. 1, pp. 7–11, Apr. 2022, doi: <https://doi.org/10.1016/j.kisu.2021.11.003>.
- [22] G. Gembillo *et al.*, “Lung Dysfunction and Chronic Kidney Disease: A Complex Network of Multiple Interactions,” *Journal of Personalized Medicine*, vol. 13, no. 2, p. 286, Feb. 2023, doi: <https://doi.org/10.3390/jpm13020286>.
- [23] A. C. M. da Silveira, Á. Sobrinho, L. D. da Silva, E. de B. Costa, M. E. Pinheiro, and A. Perkusich, “Exploring Early Prediction of Chronic Kidney Disease Using ML Algorithms for Small and Imbalanced Datasets,” *Applied Sciences*, vol. 12, no. 7, p. 3673, Apr. 2022, doi: <https://doi.org/10.3390/app12073673>.
- [24] J.-W. Ahn, S. M. Lee, and Y. H. Seo, “Factors associated with self-care behavior in patients with pre-dialysis or dialysis-dependent chronic kidney disease,” *PLOS ONE*, vol. 17, no. 10, p. e0274454, Oct. 2022, doi: <https://doi.org/10.1371/journal.pone.0274454>.
- [25] “Annual data report,” *USRDS*, 2022. <https://usrhs-adr.niddk.nih.gov/2022>
- [26] S. Vadakedath and V. Kandi, “Dialysis: A review of the mechanisms underlying complications in the management of chronic renal failure,” *Cureus*, vol. 9, no. 8, Aug. 2017, doi: <https://doi.org/10.7759/cureus.1603>.
- [27] Y. Du, A. R. Rafferty, F. M. McAuliffe, L. Wei, and C. Mooney, “An explainable ML-based clinical decision support system for prediction of gestational diabetes mellitus,” *Scientific Reports*, vol. 12, no. 1, Jan. 2022, doi: <https://doi.org/10.1038/s41598-022-05112-2>.
- [28] M. R. Afrash, A. Valinejadi, M. Amraei, and R. Noupour, “Design and implementation of an intelligent clinical decision support system for diagnosis and prediction of chronic kidney disease,” *Koomesh*, Aug. 2022, Accessed: Feb. 19, 2024. [Online]. Available: <http://eprints.lums.ac.ir/id/eprint/3907>
- [29] A. Smiti, “When ML meets medical world: Current status and future challenges,” *Computer Science Review*, vol. 37, p. 100280, Aug. 2020, doi: <https://doi.org/10.1016/j.cosrev.2020.100280>.
- [30] M. M. Baig, H. G. Hosseini, and M. Lindén, “ML-based clinical decision support system for early diagnosis from real-time physiological data,” *IEEE Xplore*, Nov. 01, 2016. <https://ieeexplore.ieee.org/document/7848584/>
- [31] S. Hong, S. Lee, J. Lee, W. C. Cha, and K. Kim, “Prediction of Cardiac Arrest in the Emergency Department Based on ML and Sequential Characteristics: Model Development and Retrospective Clinical Validation Study,” *JMIR Medical Informatics*, vol. 8, no. 8, p. e15932, Aug. 2020, doi: <https://doi.org/10.2196/15932>.
- [32] K. Chen, F. Abtahi, J.-J. Carrero, C. Fernandez-Llatas, and F. Seoane, “Process mining and data mining applications in the domain of chronic diseases: A systematic review,” *Artificial Intelligence in Medicine*, vol. 144, p. 102645, Oct. 2023, doi: <https://doi.org/10.1016/j.artmed.2023.102645>.
- [33] H. Jeong and Rishikesan Kamaleswaran, “Pivotal challenges in artificial intelligence and ML applications for neonatal care,” *Seminars in Fetal and Neonatal Medicine*, vol. 27, no. 5, pp. 101393–101393, Oct. 2022, doi: <https://doi.org/10.1016/j.siny.2022.101393>.
- [34] A. B. Hassanat, A. S. Tarawneh, S. S. Abed, G. A. Altarawneh, M. Alrashidi, and M. Alghamdi, “RDPVR: Random Data Partitioning with Voting Rule for ML from Class-Imbalanced Datasets,” *Electronics*, vol. 11, no. 2, p. 228, Jan. 2022, doi: <https://doi.org/10.3390/electronics11020228>.
- [35] L. Liu, X. Wu, S. Li, Y. Li, S. Tan, and Y. Bai, “Solving the class imbalance problem using ensemble algorithm: application of screening for aortic dissection,” *BMC Medical Informatics and Decision Making*, vol. 22, no. 1, Mar. 2022, doi: <https://doi.org/10.1186/s12911-022-01821-w>.
- [36] G. Cohen, M. Hilario, H. Sax, S. Hugonnet, and A. Geissbuhler, “Learning from imbalanced data in surveillance

- of nosocomial infection,” *Artificial Intelligence in Medicine*, vol. 37, no. 1, pp. 7–18, May 2006, doi: <https://doi.org/10.1016/j.artmed.2005.03.002>.
- [37] W. Wegier and P. Ksieniewicz, “Application of Imbalanced Data Classification Quality Metrics as Weighting Methods of the Ensemble Data Stream Classification Algorithms,” *Entropy*, vol. 22, no. 8, p. 849, Jul. 2020, doi: <https://doi.org/10.3390/e22080849>.
- [38] N. V. Chawla, K. W. Bowyer, L. O. Hall, and W. P. Kegelmeyer, “SMOTE: Synthetic Minority Over-sampling Technique,” *Journal of Artificial Intelligence Research*, vol. 16, no. 16, pp. 321–357, Jun. 2002, doi: <https://doi.org/10.1613/jair.953>.
- [39] Haibo He, Yang Bai, E. A. Garcia, and Shutao Li, “ADASYN: Adaptive synthetic sampling approach for imbalanced learning,” *IEEE Xplore*, Jun. 01, 2008, https://ieeexplore.ieee.org/abstract/document/4633969?casa_token=J_CENnbbg04AAAAA:H66LkaQgQseWdiBmYNy3Puy0nrHpFfZ7OA3Io7ZXVSCE-0_bXw-pmbIGkrE7HoIISMjkQqG7Ng
- [40] S. Barua, Md. M. Islam, X. Yao, and K. Murase, “MWMOTE--Majority Weighted Minority Oversampling Technique for Imbalanced Data Set Learning,” *IEEE Transactions on Knowledge and Data Engineering*, vol. 26, no. 2, pp. 405–425, Feb. 2014, doi: <https://doi.org/10.1109/tkde.2012.232>.
- [41] M. Mirza and S. Osindero, “Conditional Generative Adversarial Nets,” *arXiv (Cornell University)*, Nov. 2014.
- [42] L. Berger, M. Haberbush, and F. Moscato, “Generative adversarial networks in electrocardiogram synthesis: Recent developments and challenges,” *Artificial Intelligence in Medicine*, vol. 143, p. 102632, Sep. 2023, doi: <https://doi.org/10.1016/j.artmed.2023.102632>.
- [43] T. E. Raghunathan, “Synthetic Data,” *Annual Review of Statistics and Its Application*, vol. 8, no. 1, Sep. 2020, doi: <https://doi.org/10.1146/annurev-statistics-040720-031848>.
- [44] Peter X.-K. Song, “Multivariate Dispersion Models Generated From Gaussian Copula,” *Scandinavian Journal of Statistics*, vol. 27, no. 2, pp. 305–320, Jun. 2000, doi: <https://doi.org/10.1111/1467-9469.00191>.
- [45] J. A. Gallis and E. L. Turner, “Relative Measures of Association for Binary Outcomes: Challenges and Recommendations for the Global Health Researcher,” *Annals of Global Health*, vol. 85, no. 1, 2019, doi: <https://doi.org/10.5334/aogh.2581>.
- [46] W. Zhou, M. Kroehl, M. Meier, and A. Kaizer, “Approaches to analyzing binary data for large-scale A/B testing,” *Contemporary Clinical Trials Communications*, vol. 32, p. 101091, Apr. 2023, doi: <https://doi.org/10.1016/j.conctc.2023.101091>.
- [47] F. J. Valverde-Albacete and C. Peláez-Moreno, “100% Classification Accuracy Considered Harmful: The Normalized Information Transfer Factor Explains the Accuracy Paradox,” *PLoS ONE*, vol. 9, no. 1, p. e84217, Jan. 2014, doi: <https://doi.org/10.1371/journal.pone.0084217>.
- [48] S. Liao, C. Song, X. Wang, and Y. Wang, “A classification framework for identifying bronchitis and pneumonia in children based on a small-scale cough sounds dataset,” *PLOS ONE*, vol. 17, no. 10, pp. e0275479–e0275479, Oct. 2022, doi: <https://doi.org/10.1371/journal.pone.0275479>.
- [49] Y. Zhao, Z. S.-Y. Wong, and K. L. Tsui, “A Framework of Rebalancing Imbalanced Healthcare Data for Rare Events’ Classification: A Case of Look-Alike Sound-Alike Mix-Up Incident Detection,” *Journal of Healthcare Engineering*, vol. 2018, pp. 1–11, 2018, doi: <https://doi.org/10.1155/2018/6275435>.
- [50] S. A. Hicks *et al.*, “On evaluation metrics for medical applications of artificial intelligence,” *Scientific Reports*, vol. 12, no. 1, p. 5979, Apr. 2022, doi: <https://doi.org/10.1038/s41598-022-09954-8>.
- [51] H. Chen, N. Wang, X. Du, K. Mei, Y. Zhou, and G. Cai, “Classification Prediction of Breast Cancer Based on ML,” *Computational Intelligence and Neuroscience*, vol. 2023, pp. 1–9, Jan. 2023, doi: <https://doi.org/10.1155/2023/6530719>.
- [52] M. Dorado-Moreno, M. Prez-Ortiz, P. A. Gutierrez, R. Ciria, J. Briceo, and Csar Hervs-Martnez, “Dynamically weighted evolutionary ordinal neural network for solving an imbalanced liver transplantation problem,” *Artificial Intelligence in Medicine*, vol. 77, pp. 1–11, Mar. 2017, doi: <https://doi.org/10.1016/j.artmed.2017.02.004>.
- [53] B. Krawczyk, G. Schaefer, and M. Woźniak, “A hybrid cost-sensitive ensemble for imbalanced breast thermogram classification,” *Artificial Intelligence in Medicine*, vol. 65, no. 3, pp. 219–227, Nov. 2015, doi: <https://doi.org/10.1016/j.artmed.2015.07.005>.
- [54] X. Gao, S. Alam, P. Shi, F. Dexter, and N. Kong, “Interpretable ML models for hospital readmission prediction: a two-step extracted regression tree approach,” *BMC Medical Informatics and Decision Making*, vol. 23, no. 1, Jun. 2023, doi: <https://doi.org/10.1186/s12911-023-02193-5>.
- [55] T. Razzaghi, I. Safro, J. Ewing, E. Sadrfaridpour, and J. D. Scott, “Predictive models for bariatric surgery risks with imbalanced medical datasets,” *Annals of Operations Research*, vol. 280, no. 1–2, pp. 1–18, Feb. 2019, doi: <https://doi.org/10.1007/s10479-019-03156-8>.
- [56] T. Liu, W. Fan, and C. Wu, “A hybrid ML approach to cerebral stroke prediction based on imbalanced medical

- dataset,” *Artificial Intelligence in Medicine*, vol. 101, p. 101723, Nov. 2019, doi: <https://doi.org/10.1016/j.artmed.2019.101723>.
- [57] Z. Xu, D. Shen, T. Nie, and Y. Kou, “A hybrid sampling algorithm combining M-SMOTE and ENN based on Random forest for medical imbalanced data,” *Journal of Biomedical Informatics*, vol. 107, p. 103465, Jul. 2020, doi: <https://doi.org/10.1016/j.jbi.2020.103465>.
- [58] Y. Hirano *et al.*, “ML Approach to Predict Positive Screening of Methicillin-Resistant Staphylococcus aureus During Mechanical Ventilation Using Synthetic Dataset From MIMIC-IV Database,” *Frontiers in Medicine*, vol. 8, Nov. 2021, doi: <https://doi.org/10.3389/fmed.2021.694520>.
- [59] X. Shi, T. Qu, Gijs Van Pottelbergh, van, and Bart De Moor, “A Resampling Method to Improve the Prognostic Model of End-Stage Kidney Disease: A Better Strategy for Imbalanced Data,” *Frontiers in Medicine*, vol. 9, Mar. 2022, doi: <https://doi.org/10.3389/fmed.2022.730748>.
- [60] R. Hassanzadeh, M. Farhadian, and H. Rafieemehr, “Hospital mortality prediction in traumatic injuries patients: comparing different SMOTE-based ML algorithms,” *BMC Medical Research Methodology*, vol. 23, no. 1, Apr. 2023, doi: <https://doi.org/10.1186/s12874-023-01920-w>.
- [61] Nicholas I-Hsien Kuo *et al.*, “Generating synthetic clinical data that capture class imbalanced distributions with generative adversarial networks: Example using antiretroviral therapy for HIV,” *Journal of Biomedical Informatics*, vol. 144, pp. 104436–104436, Aug. 2023, doi: <https://doi.org/10.1016/j.jbi.2023.104436>.
- [62] A. J. Rodriguez-Almeida *et al.*, “Synthetic Patient Data Generation and Evaluation in Disease Prediction Using Small and Imbalanced Datasets,” *IEEE Journal of Biomedical and Health Informatics*, vol. 27, no. 6, pp. 1–12, 2022, doi: <https://doi.org/10.1109/jbhi.2022.3196697>.
- [63] X. Chen, H. Chen, S. Nan, X. Kong, H. Duan, and H. Zhu, “Dealing With Missing, Imbalanced, and Sparse Features During the Development of a Prediction Model for Sudden Death Using Emergency Medicine Data: ML Approach,” *JMIR Medical Informatics*, vol. 11, p. e38590, Jan. 2023, doi: <https://doi.org/10.2196/38590>.
- [64] X. Weng *et al.*, “A joint learning method for incomplete and imbalanced data in electronic health record based on generative adversarial networks,” *Computers in Biology and Medicine*, vol. 168, pp. 107687–107687, Jan. 2024, doi: <https://doi.org/10.1016/j.compbiomed.2023.107687>.
- [65] Y. Lu *et al.*, “Risk factor mining and prediction of urine protein progression in chronic kidney disease: a ML-based study,” *BMC Medical Informatics and Decision Making*, vol. 23, no. 1, Aug. 2023, doi: <https://doi.org/10.1186/s12911-023-02269-2>.
- [66] H.-H. Chang, J.-H. Chiang, C.-C. Tsai, and P.-F. Chiu, “Predicting hyperkalemia in patients with advanced chronic kidney disease using the XGBoost model,” *BMC Nephrology*, vol. 24, no. 1, Jun. 2023, doi: <https://doi.org/10.1186/s12882-023-03227-w>.
- [67] Z. Ye *et al.*, “The prediction of in-hospital mortality in chronic kidney disease patients with coronary artery disease using ML models,” *European Journal of Medical Research*, vol. 28, no. 1, Jan. 2023, doi: <https://doi.org/10.1186/s40001-023-00995-x>.
- [68] A. Kawalec *et al.*, “Systemic Immune Inflammation Index as a Key Predictor of Dialysis in Pediatric Chronic Kidney Disease with the Use of Random Forest Classifier,” *Journal of Clinical Medicine*, vol. 12, no. 21, pp. 6911–6911, Nov. 2023, doi: <https://doi.org/10.3390/jcm12216911>.
- [69] M. M. Klamrowski *et al.*, “Short Timeframe Prediction of Kidney Failure among Patients with Advanced Chronic Kidney Disease,” *Clinical Chemistry*, vol. 69, no. 10, pp. 1163–1173, Jul. 2023, doi: <https://doi.org/10.1093/clinchem/hvad112>.
- [70] J. Aoki *et al.*, “CKD Progression Prediction in a Diverse US Population: A Machine-Learning Model,” *Kidney Medicine*, vol. 5, no. 9, pp. 100692–100692, Sep. 2023, doi: <https://doi.org/10.1016/j.xkme.2023.100692>.
- [71] Jakub Stojanowski *et al.*, “The Artificial Neural Network as a Diagnostic Tool of the Risk of Clostridioides difficile Infection among Patients with Chronic Kidney Disease,” *Journal of Clinical Medicine*, vol. 12, no. 14, pp. 4751–4751, Jul. 2023, doi: <https://doi.org/10.3390/jcm12144751>.
- [72] P. Liang *et al.*, “Deep Learning Identifies Intelligible Predictors of Poor Prognosis in Chronic Kidney Disease,” *IEEE Journal of Biomedical and Health Informatics*, vol. 27, no. 7, pp. 3677–3685, Jul. 2023, doi: <https://doi.org/10.1109/jbhi.2023.3266587>.
- [73] Z. A. Massy *et al.*, “ML-Based Urine Peptidome Analysis to Predict and Understand Mechanisms of Progression to Kidney Failure,” *Kidney International Reports*, vol. 8, no. 3, pp. 544–555, Mar. 2023, doi: <https://doi.org/10.1016/j.ekir.2022.11.023>.
- [74] P. Yan, B. Ke, J. Song, and X. Fang, “Identification of immune-related molecular clusters and diagnostic markers in chronic kidney disease based on cluster analysis,” *Frontiers in Genetics*, vol. 14, Feb. 2023, doi: <https://doi.org/10.3389/fgene.2023.1111976>.
- [75] M. B. Kursu and W. R. Rudnicki, “Feature Selection with the Boruta Package,” *Journal of Statistical Software*,

- vol. 36, no. 11, 2010, doi: <https://doi.org/10.18637/jss.v036.i11>.
- [76] M. Sundararajan, A. Taly, and Q. Yan, "Axiomatic attribution for deep networks," in *ICML '17: Proceedings of the 34th International Conference on ML*, Aug. 2017, pp. 3319–3328.
- [77] S. Cuschieri, "The STROBE guidelines," *Saudi Journal of Anaesthesia*, vol. 13, no. 5, p. 31, 2019, doi: https://doi.org/10.4103/sja.sja_543_18.
- [78] M. Amiri Shahbazi, "Developing Artificial Intelligence tools to investigate the phenotypes and correlates of Chronic Kidney Disease patients in West Virginia," *Graduate Theses, Dissertations, and Problem Reports*, Jan. 2022, doi: <https://doi.org/10.33915/etd.11481>.
- [79] K. Makris and L. Spanou, "Acute Kidney Injury: Definition, Pathophysiology and Clinical Phenotypes," *The Clinical biochemist. Reviews*, vol. 37, no. 2, pp. 85–98, May 2016, Available: <https://www.ncbi.nlm.nih.gov/pmc/articles/PMC5198510/>
- [80] M. D. Breyer and K. Susztak, "THE NEXT GENERATION OF THERAPEUTICS FOR CHRONIC KIDNEY DISEASE," *Nature reviews. Drug discovery*, vol. 15, no. 8, pp. 568–588, Aug. 2016, doi: <https://doi.org/10.1038/nrd.2016.67>.
- [81] "Work Group Membership," *Kidney International Supplements*, vol. 2, no. 1, p. 2, Mar. 2012, doi: <https://doi.org/10.1038/kisup.2012.2>.
- [82] A. Ali, C. Bhan, M. B. Malik, M. Q. Ahmad, and S. A. Sami, "The Prevention and Management of Contrast-induced Acute Kidney Injury: A Mini-review of the Literature," *Cureus*, vol. 10(9), Sep. 2018, doi: <https://doi.org/10.7759/cureus.3284>.
- [83] A. E. Maxwell, T. A. Warner, and L. A. Guillén, "Accuracy Assessment in Convolutional Neural Network-Based Deep Learning Remote Sensing Studies—Part 2: Recommendations and Best Practices," *Remote Sensing*, vol. 13, no. 13, p. 2591, Jul. 2021, doi: <https://doi.org/10.3390/rs13132591>.
- [84] A. E. Maxwell and T. A. Warner, "Thematic Classification Accuracy Assessment with Inherently Uncertain Boundaries: An Argument for Center-Weighted Accuracy Assessment Metrics," *Remote Sensing*, vol. 12, no. 12, p. 1905, Jun. 2020, doi: <https://doi.org/10.3390/rs12121905>.
- [85] Basim Ahmad Alabsi, M. Anbar, and A. Rihan, "Conditional Tabular Generative Adversarial Based Intrusion Detection System for Detecting Ddos and Dos Attacks on the Internet of Things Networks," *Sensors*, vol. 23, no. 12, pp. 5644–5644, Jun. 2023, doi: <https://doi.org/10.3390/s23125644>.
- [86] Mei Ling Fang, Devendra Singh Dhami, and K. Kersting, "DP-CTGAN: Differentially Private Medical Data Generation Using CTGANs," *Lecture Notes in Computer Science*, vol. 13263, pp. 178–188, Jan. 2022, doi: https://doi.org/10.1007/978-3-031-09342-5_17.
- [87] S. R. Malakshan, M. S. E. Saadabadi, M. Mostofa, S. Soleymani, and N. M. Nasrabadi, "Joint Super-Resolution and Head Pose Estimation for Extreme Low-Resolution Faces," *IEEE Access*, vol. 11, pp. 11238–11253, 2023, doi: <https://doi.org/10.1109/access.2023.3241606>.
- [88] A. S. Dina, A. B. Siddique, and D. Manivannan, "Effect of Balancing Data Using Synthetic Data on the Performance of ML Classifiers for Intrusion Detection in Computer Networks," *IEEE Access*, vol. 10, pp. 96731–96747, 2022, doi: <https://doi.org/10.1109/access.2022.3205337>.
- [89] Ferdib-Al-Islam and M. Ghosh, "An Enhanced Stroke Prediction Scheme Using SMOTE and ML Techniques," *12th International Conference on Computing Communication and Networking Technologies (ICCCNT)*, Jul. 2021, doi: <https://doi.org/10.1109/icccnt51525.2021.9579648>.
- [90] E. Ileberi, Y. Sun, and Z. Wang, "Performance Evaluation of ML Methods for Credit Card Fraud Detection Using SMOTE and AdaBoost," *IEEE Access*, vol. 9, pp. 165286–165294, 2021, doi: <https://doi.org/10.1109/access.2021.3134330>.
- [91] Sklar, A. (1959) Fonctions de Répartition à n Dimensions et Leurs Marges. Publications de l'Institut Statistique de l'Université de Paris, 8, 229-231.
- [92] D. Meyer, T. Nagler, and R. J. Hogan, "Copula-based synthetic data augmentation for machine-learning emulators," *Geoscientific Model Development*, vol. 14, no. 8, pp. 5205–5215, Aug. 2021, doi: <https://doi.org/10.5194/gmd-14-5205-2021>.
- [93] Diogo Filipe Pereira, Fontes Fernandes Silva, S. Leonhardt, and Christoph Hoog Antink, "Synthesis of cardiac signals using a Copula-approach," *AIP Conference Proceedings*, vol. 2140, no. 1, Jan. 2019, doi: <https://doi.org/10.1063/1.5121995>.
- [94] H. Lin and N. R. Chaganty, "Multivariate distributions of correlated binary variables generated by pair-copulas," *Journal of Statistical Distributions and Applications*, vol. 8, no. 1, Mar. 2021, doi: <https://doi.org/10.1186/s40488-021-00118-z>.
- [95] T. P. Ryan, *Modern engineering statistics*. Hoboken: Wiley-Interscience, Cop, 2007.
- [96] S. Das, H. N. Mhaskar, and A. Cloninger, "Kernel Distance Measures for Time Series, Random Fields and Other

Structured Data,” *Frontiers in Applied Mathematics and Statistics*, vol. 7, Dec. 2021, doi: <https://doi.org/10.3389/fams.2021.787455>.

[97] A. Potapov *et al.*, “PT-MMD: A Novel Statistical Framework for the Evaluation of Generative Systems,” 2019, 2219-2223. Doi: 10.1109/IEEECONF44664.2019.9048757.